This article has been accepted for publication in a future issue of this journal, but has not been fully edited. Content may change prior to final publication.
Citationinformation: DOI: 10.1109/TWC.2025.3581097, IEEE Transactions on Wireless Communications

Wireless-powered Multi-access Edge Computing with Cascaded zeRISs

Luyao Zhang, Yi Zhou, *Member, IEEE,* Sotiris A. Tegos, *Senior Member, IEEE,* Yu Zheng, Panagiotis D. Diamantoulakis, *Senior Member, IEEE,* Li Hao, *Member, IEEE,* George K. Karagiannidis, *Fellow, IEEE*

***Abstract*—In this paper, we develop an energy minimization framework for wireless-powered multi-access edge computing (WP-MEC) networks, where two zero-energy reconfigurable intelligent surfaces (zeRISs) are employed to support energy harvesting and task offloading. In the downlink energy harvesting period, the hybrid access point (HAP) provides energy beamforming for multiple zero-energy devices and two zeRISs, where the harvested energy is used to offload tasks in the uplink period. Specifically, an optimization problem is formulated to minimize the energy consumption at the HAP, jointly considering the nonlinear energy harvesting model and the cascaded RIS link. Next, an efficient iterative solution is designed to realize joint time allocation, HAP energy beamforming, and reflection coefficients for two-RIS by employing alternating optimization and semidefinite relaxation methods. Numerical results demonstrate the superiority of the algorithm. Compared to the corresponding single RIS setup, the energy consumption of the HAP under the proposed two-zeRIS scheme is significantly reduced.**

***Index Terms*—Reconfigurable intelligent surfaces (RISs), wireless powered multi-access edge computing (WP-MEC), nonlinear energy harvesting, zero-energy devices (ZEDs), alternating optimization (AO) algorithm.**

I. Introduction

With the rapid development of sixth generation (6G) wireless networks, massive immersive and innovative applications, such as virtual reality, remote healthcare, and smart home management can be accessed promptly and easily via smart devices [1]. However, these advanced applications may potentially result in high power consumption; thus, how to charge the power-limited devices and tablets flexibly and rapidly presents a significant challenge in 6G networks. To tackle this difficulty, wireless power transfer (WPT), which offers a new mode for zero-energy devices (ZEDs) delivering power without traditional batteries, has become one strong technical enabler [2]. ZEDs harvest energy from the environment and operate intermittently, eliminating the need for batteries or manual charging to operate. Unlike information decoding, WPT technology primarily focuses on effective energy transmission [3], [4]. It is noted that WPT has been a well-investigated topic in the last decade, and several fundamental contributions have been made. Indicatively, the authors in [5] introduced a two-stage water-filling energy scheduling scheme in an energy harvesting-driven device-to-device relay network. Moreover, the authors in [6] investigated a WPT system utilizing a large-scale antenna array, where the effective range of WPT can be widely extended. However, due to the significant distance-dependent attenuation, power-constrained edge devices can only harvest a small portion of the transmitted energy, limiting the charging performance.

To support the harvesting process, reconfigurable intelligent surfaces (RISs), which provide strong energy beamforming gain by intelligently adjusting the reflection coefficient [7], were used to reconstruct the wireless channels between the transceivers and reduce power consumption at the source [8], [9]. With the help of RISs, not only the network capacity but also the energy efficiency in WPT networks can be greatly improved [10]–[12]. The work in [13] analyzed the effects of reflection coefficient errors and hardware imperfections in transceivers on RIS-supported wireless-powered Internet of Things networks. In addition, [14] also used a RIS to support WPT networks due to the passive beamforming gain of the RIS. More recently, zero-energy RIS (zeRIS), capable of absorbing energy from an external energy supply, has attracted increasing attention in WPT networks [15], [16]. In [15], a zero-energy RIS is used to harvest energy from a HAP to sustain its operation. The work in [16] presented an efficient solution that meets the power demands of energy devices and RIS in synchronized terahertz information and power transmission systems. Deploying multiple distributed RISs can significantly enhance performance compared to a single RIS [17], the use of double RISs under a cascaded RIS system is expected to enhance system performance by reducing energy consumption through the introduction of cascaded reflection links [18]. However, when the number of RISs increases to three, the resulting path loss exceeds the beamforming gain achieved by the cascaded RIS system as a result of the path loss term's multiplicative effect [19].

On the other hand, multi-access edge computing (MEC) also known as mobile edge computing, which enables devices to offload tasks to edge servers via wireless channels, is another important technology in 6G networks [20]. In the context of

This work was supported in part by the National Key R&D Program of China under Grant 2023YFB2603500, in part by the National Natural Science Foundation of China under Grant 62361136810 and 62301462, and in part by NSFC 62350710217, international cooperation project S20240364 and Sichuan HT 2024JDHJ0042. (Corresponding author: Yi Zhou (email: yizhou@swjtu.edu.cn).)

Luyao Zhang, Yi Zhou, and Li Hao are with the Provincial Key Laboratory of Information Coding and Transmission, Southwest Jiaotong University, Chengdu 610031, China (e-mails: zhangly@my.swjtu.edu.cn; yizhou@swjtu.edu.cn; lhao@swjtu.edu.cn).

Yu Zheng is with the Department of automation, Tsinghua University, Beijing 100084, China (e-mail: zheng-yu@mails.tsinghua.edu.cn).

S. A. Tegos, P. D. Diamantoulakis, and G. K. Karagiannidis are with the Electrical and Computer Engineering Department, Aristotle University of Thessaloniki, 54124 Thessaloniki, Greece and also with the Provincial Key Laboratory of Information Coding and Transmission, Southwest Jiaotong University, Chengdu 610031, China (e-mails: tegosoti@auth.gr; padiaman@auth.gr; geokarag@auth.gr).

This article has been accepted for publication in a future issue of this journal, but has not been fully edited. Content may change prior to final publication.
Citation information: DOI: 10.1109/TWC.2025.3581097, IEEE Transactions on Wireless Communications

RIS-assisted MEC systems, several noteworthy works have focused on minimizing the energy and operational cost [21]–[25]. In [21] and [22], a single RIS was utilized to adjust the wireless propagation environment and enhance transmission rates in offloading links. With the goal of minimizing energy consumption across all user equipment (UEs), the authors in [24] studied a scalable resource scheduling algorithm for unmanned aerial vehicle (UAV)-enabled RIS-assisted dynamic MEC systems. The security performance of the RIS-MEC system was discussed in [25], where one RIS was deployed to strengthen the user's signal while weakening the eavesdropper's signal. Moreover, the latency and throughput performance in RIS-assisted MEC systems was investigated in [26]–[28]. In particular, the authors in [27] considered minimizing the offloading delay by jointly optimizing the channel allocation, beamwidth allocation, offloading rate, and power control. To further enhance the offloading capability, two RISs were deployed to speed up the offloading rate where the cascaded link between RISs was considered [29].

Embedding WPT in MEC networks is appealing because the power limitations of edge devices can be well compensated. The applications enabled by WP-MEC fall into three main categories: Internet of Things (IoT) networks, wireless sensor networks, and smart grids. In [30], wireless devices receive energy through WPT from an AP, enabling them to process the computational tasks locally or offload them to an edge server. To achieve additional energy savings, the authors minimized the HAP's total energy by jointly optimizing energy transfer beamforming and computing resource allocation at the HAP. To realize the self-sustainability of mobile devices, the authors in [31] integrated WPT into MEC systems and proposed an energy-saving computing framework. However, when the wireless channel between HAP and UE is blocked, the efficiency of WPT and task offloading in wireless powered mobile edge computing (WP-MEC) significantly drops [32]. To tackle this issue, the authors in [33], [34] considered deploying RIS around the devices to provide additional transmission paths for wireless power transfer and computing task offloading. Moreover, the works in [35], [36] verified that deploying RISs can effectively increase the overall computing rate in the WP-MEC system.

A. Motivation and Contributions

Although studies on RIS-assisted WP-MEC have been investigated in [32]–[39], these works have overlooked the importance of the power consumption used for the reflection coefficient, which is crucial for understanding the self-sustainability of WP-MEC. However, if certain devices are positioned within the signal dead zones, the deployment of a single RIS cannot guarantee the computation offloading rate in RIS-assisted WP-MEC networks. While a single zero-energy RIS has been used in [15], [16] to improve the power transfer performance, whether the WPT and communication performance can be further improved, aided by the internal beamforming gain between two cascaded zeRISs with reduced energy consumption, has not been thoroughly discussed. In such cases, the use of multiple RISs for energy harvesting and task offloading is urgently needed. Moreover, although multiple RISs were deployed in [40], [41], these works addressed distributed RISs to assist the energy harvesting and task offloading, whether the consumed energy can be further minimized aided by double RISs with cascaded link is unknown. Unfortunately, the authors in [40], [41] have overlooked the importance of the power consumption used for the reflection coefficient, which is crucial for achieving the self-sustainability of WP-MEC. In Table I, we summarized the key features of the existing research, and observed that no previous work has discussed the energy minimization problem in a WP-MEC system with zeRISs, which motivates this work.

To fill the above gap, in this work, we develop an advanced WP-MEC framework supported by two zeRISs for zero-energy MEC networks with higher coverage. However, realizing minimizing the energy that is consumed by the HAP despite the complexity of the considered scenario is challenging. The first primary challenge in this paper is how to effectively minimize the HAP's total energy consumption by jointly optimizing the time allocation, reflection coefficient matrices for zeRISs , HAP energy beamforming in downlink (DL), HAP reception beamforming in uplink (UL), and device transmit power allocation in UL, where all variables are strongly coupled in the optimization. Moreover, since a practical nonlinear harvesting model is adopted in the DL phase, solving the beamforming of HAP and reflection coefficient matrices for the RISs is difficult due to the nonlinearity. In addition, with cascaded links between RISs, it is more challenging to solve the corresponding reflection coefficients due to the strengthened coupling effect. To address these difficulties, several mathematical solutions, including alternating optimization (AO) and semi-definite relaxation (SDR), are employed, and an iterative energy minimization algorithm is developed. We highlight the main contributions of this work as follows:

- An energy minimization framework is developed in zeRIS-aided WP-MEC systems, considering two zeRISs, the existence of a cascaded zeRIS link, and nonlinear harvesting model. In the DL energy harvesting period, the HAP provides energy beamforming for multiple ZEDs and double RISs, where the harvested energy is used to offload the task in the UL period.
- To address the non-convex nature of the formulated problem, we designed an algorithm that iteratively minimizes energy by optimizing the time allocation, HAP energy beamforming, HAP receive beamforming, and joint reflection coefficients design of two zeRISs variables via AO, SDR, and mathematical solutions.
- The numerical results confirm the significant benefits of adopting two zeRISs in WP-MEC systems on energy minimization. A series of quantitative evaluations and a comparative analysis with existing benchmark solutions were investigated.

B. Paper Outline and Notation

The remainder of this manuscript is structured as follows. Section II provides a detailed discussion of the double zeRIS-empowered WP-MEC system model. In Section III, we introduce efficient algorithms designed to address the challenges

This article has been accepted for publication in a future issue of this journal, but has not been fully edited. Content may change prior to final publication.
Citation information: DOI: 10.1109/TWC.2025.3581097, IEEE Transactions on Wireless Communications

TABLE I: Comparisons between this work and relevant literature

Reference	RISs	Multi-antenna AP	Nonlinear energy harvest	Zero-energy RIS	WP-MEC
[32], [33], [35], [39]	×	×	×	×	✓
[34]	×	×	✓	×	✓
[36]	×	×	×	✓	✓
[40]	✓	✓	×	×	✓
[38]	×	✓	×	✓	✓
[18]	✓	✓	✓	×	×
Proposed	✓	✓	✓	✓	✓

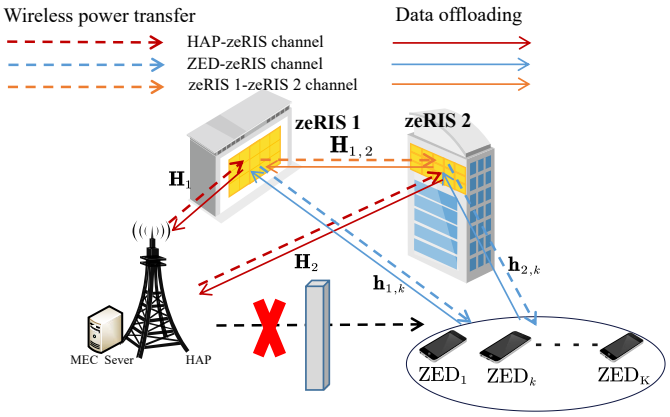

Fig. 1: Energy-minimization framework in zeRIS-aided WP-MEC system.

presented in the formulated problems, particularly focusing on the double zeRISs cooperative system. The numerical results of these investigations are systematically presented in Section IV. Finally, we present the conclusion of our research in Section V.

Notation: Boldface (lower case) $\mathbf{x}$ represents vectors, (upper case) $\mathbf{X}$ denotes matrices, and scalars are indicated by lower-case letters. Let $\mathbf{X}^T$, $\mathbf{X}^H$, diag($\mathbf{X}$), and $\mathrm{tr}(\mathbf{X})$ represent the transpose, the conjugate transpose, diagonalization, and trace of $\mathbf{X}$, respectively. $\mathbf{X}_{i,j}$ denotes the (i,j)-th entry of matrix $\mathbf{X}$. $\mathbf{X}_1 \succeq 0$ means that $\mathbf{X}_1$ is a positive semi-definite matrix. $\mathbb{C}$ and $\mathbb{E}\{\cdot\}$ denote the complex matrix and the expectation operator. A circularly symmetric complex Gaussian (CSCG) random vector $\mathbf{m}$ is denoted $\mathbf{m} \sim \mathcal{CN}(\bar{\mathbf{m}}, \mathbf{Q})$, where $\bar{\mathbf{m}}$ is the mean and $\mathbf{Q}$ is the covariance matrix. $\mathbf{I}$ represents an identity matrix.

II. System Model

As shown in Fig. 1, a zeRIS-aided WP-MEC system is considered, which consists of a HAP equipped with M antennas embedded with an edge server, K single-antenna devices, and two zeRISs (each zeRIS is equipped with N elements). ZeRIS 1 is deployed near the multi-antenna HAP, while zeRIS 2 is positioned near the center of the device cluster, thereby increasing the overall network coverage. Specifically, in the DL energy harvesting period, both devices and zeRISs adopt a nonlinear harvesting model to achieve self-sustainability. The ZEDs use the harvested energy to offload tasks with the help of zeRISs in the UL period. This procedure consists of the following two stages:

- Stage 1: During the configuration stage, the BS optimizes the resource allocation parameters using a centralized optimization entity, based on the acquired channel state information. The optimal values of the resource allocation parameters are then reported back to the RISs and ZEDs.
- Stage 2: As shown in Fig. 2, the second stage consists of two different phases, i.e., the wireless power transfer phase and the computing offloading phase. More details about the two transmission phases are provided below:
  1) During the wireless power transfer phase, the HAP transmits energy signals to devices and zeRISs. The zeRISs use part of the signal to perform energy harvesting and the rest is reflected to the devices.
  2) During the computing offloading phase, each ZED can use the harvested energy to offload its tasks to the HAP. Since the devices may lack sufficient energy to perform local processing effectively, and inspired by [42], we consider that the power-limited devices offload all task and the server performs the computation after receiving it and returns the calculation results to the devices. Thus, all devices use the harvested energy to offload tasks to the HAP via single-reflection and cascaded links.

It should be noted that the two phases of the second stage are implemented using time-division duplexing, and channel reciprocity is assumed. Thus, the HAP performs channel estimation using pilots transmitted by the users in the uplink. In addition, a different set of RIS reflection coefficients is optimized for each transmission phase. While this requires control signaling to update the RIS configurations, the signaling overhead is limited because the RIS elements are adjusted via a central controller using low-rate control channels, in accordance with the processes performed in the first stage.

By jointly optimizing the amplitude coefficients and phase shifts of the RISs, the RISs absorb part of the energy to maintain self-sustainability. In contrast, the other part is reflected to the ZEDs. The information reflection coefficients for the r-th zeRIS in the UL are given by

$$\boldsymbol{\theta}_r^{ul} \triangleq [\beta_{r,1}^{ul}\theta_{r,1}^{ul}, \ldots, \beta_{r,n}^{ul}\theta_{r,n}^{ul}, \ldots, \beta_{r,N}^{ul}\theta_{r,N}^{ul}]^T. \quad (1)$$

Let

$$\boldsymbol{\theta}_r^{dl} \triangleq [\beta_{r,1}^{dl}\theta_{r,1}^{dl}, \ldots, \beta_{r,n}^{dl}\theta_{r,n}^{dl}, \ldots, \beta_{r,N}^{dl}\theta_{r,N}^{dl}], \quad (2)$$

This article has been accepted for publication in a future issue of this journal, but has not been fully edited. Content may change prior to final publication.
Citation information: DOI: 10.1109/TWC.2025.3581097, IEEE Transactions on Wireless Communications

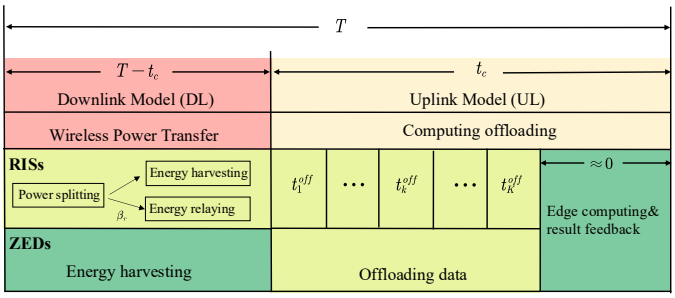

Fig. 2: Transmission phase (stage 2).

represent the energy reflection coefficients for the r-th RIS in the DL, where $\beta_{r,n}^{ul/dl} \in (0,1)$ and $\theta_{r,n}^{ul/dl} \in [0, 2\pi)$ are the reflective amplitudes and the phase shifts of the n-th element of r-th RIS, respectively. Then we have the following constraint,

$$\left|\beta_{r,n}^{ul/dl} e^{j\theta_{r,n}^{ul/dl}}\right| \leqslant 1, \quad \forall n,\ r \in \{1,2\}. \tag{3}$$

A. Channel Model

The equivalent DL channels include the HAP to the r-th RIS channel $\mathbf{H}_r \in \mathbb{C}^{N\times M}$, the RIS 1 to RIS 2 channel $\mathbf{H}_{1,2} \in \mathbb{C}^{N\times N}$, and the r-th RIS to the k-th ZED channel $\mathbf{h}_{r,k}^H \in \mathbb{C}^{1\times N}$, where $r \in \{1,2\}$. We consider that the obstacles block the direct links between the k-th ZED and the HAP. Moreover, assuming channel reciprocity and block-fading, the channel state information (CSI) for both UL and DL is considered to remain constant within a period [42]. Regarding the channel estimation, it can be efficiently performed by using the method presented in [43], which is appropriate for estimating the cascaded CSI for the proposed cooperative zeRISs system. In addition, the channel estimation algorithms in [44] and [45] can be considered for imperfect CSI. Thus, the equivalent UL channels include the k-th ZED to the r-th RIS channel $\mathbf{h}_{r,k} \in \mathbb{C}^{N\times 1}$, the RIS 2 to RIS 1 channel $\mathbf{H}_{1,2}^H \in \mathbb{C}^{N\times N}$, and the r-th RIS to the HAP channel $\mathbf{H}_r^H \in \mathbb{C}^{M\times N}$, where $r \in \{1,2\}$. Under this configuration, the channel between the HAP and the k-th ZED consists of three cascade channels (i.e., HAP→RIS 1→k-th ZED channel, HAP→RIS 2→k-th ZED channel, and HAP→RIS 1→RIS 2→k-th ZED channel). The latter provides additional degrees of freedom (DoF), particularly useful in environments with obstacles [12], [29], [46]. The use of the above links can be configured by the appropriately designed codebooks that are utilized by the microcontroller in each RIS. It should be noted that the cascaded link (HAP→RIS 2→RIS 1→k-th ZED) is omitted due to its higher path loss [12], [29].

All links are assumed to follow Rician fading [29],where the channel $\mathbf{X} \in \{\mathbf{H}_r, \mathbf{H}_{1,2}, \mathbf{h}_{r,k}\}$, $r \in \{1,2\}$ is given by

$$\mathbf{X} = \sqrt{\frac{\omega}{\omega+1}}\mathbf{X}^{LoS} + \sqrt{\frac{1}{\omega+1}}\mathbf{X}^{NLoS}, \tag{4}$$

with ω, $\mathbf{X}^{LoS}$, and $\mathbf{X}^{NLoS}$ being the Rician factor, the line-of-sight (LoS) component, and the non-line-of-sight (NLoS) component of the channel, respectively.

Let $\mathbf{\Theta}_r^{ul}$ and $\mathbf{\Theta}_r^{dl}$ denote the UL and DL reflection coefficient matrices of the r-th zeRIS, respectively, where $r \in \{1,2\}$. Specifically,

$$\mathbf{\Theta}_r^{ul} = \mathrm{diag}(\boldsymbol{\theta}_r^{ul}) \in \mathbb{C}^{N\times N}, \quad \mathbf{\Theta}_r^{dl} = \mathrm{diag}(\boldsymbol{\theta}_r^{dl}) \in \mathbb{C}^{N\times N}.$$

Let $\mathbf{\Psi}_k$ and $\mathbf{\Phi}_k$, represent the UL and DL estimated channel covariance matrices, respectively. Thus, for the k-th ZED, the UL and DL channel covariance matrices are given by

$$\mathbf{\Psi}_k = \mathbb{E}\left\{\mathbf{\Omega}_k^{ul}\left(\mathbf{\Omega}_k^{ul}\right)^H\right\} \in \mathbb{C}^{M\times M}, \tag{5}$$

and

$$\mathbf{\Phi}_k = \mathbb{E}\left\{\left(\mathbf{\Omega}_k^{dl}\right)^H \mathbf{\Omega}_k^{dl}\right\} \in \mathbb{C}^{M\times M}, \tag{6}$$

where

$$\mathbf{\Omega}_k^{ul} = \mathbf{H}_1^H \mathbf{\Theta}_1^{ul} \mathbf{H}_{1,2}^H \mathbf{\Theta}_2^{ul} \mathbf{h}_{2,k} + \mathbf{H}_1^H \mathbf{\Theta}_1^{ul} \mathbf{h}_{1,k} + \mathbf{H}_2^H \mathbf{\Theta}_2^{ul} \mathbf{h}_{2,k},$$

and

$$\mathbf{\Omega}_k^{dl} = \mathbf{h}_{2,k}^H \mathbf{\Theta}_2^{dl} \mathbf{H}_{1,2} \mathbf{\Theta}_1^{dl} \mathbf{H}_1 + \mathbf{h}_{1,k}^H \mathbf{\Theta}_1^{dl} \mathbf{H}_1 + \mathbf{h}_{2,k}^H \mathbf{\Theta}_2^{dl} \mathbf{H}_2.$$

B. Wireless Power Transfer

As depicted in Fig. 2, the time allocated to the DL is $T - t_c$ ($0 \leq t_c < T$). All devices harvest energy through the DL channel during the entire WPT phase. RISs employ a power-splitting (PS) scheme to assist the WPT and modulate the amplitude reflection coefficients $\beta_{r,n}^{dl}$. The PS scheme enhances energy harvesting efficiency by allocating part of the HAP energy signal to maintain the self-sustainability of each RIS, and the remaining part is reflected to support the ZEDs [15]. Furthermore, RIS 1 harvests energy through the channel $\mathbf{H}_1$, and RIS 2 harvests energy through the channel $\widehat{\mathbf{H}}_2 = \mathbf{H}_{1,2}\mathbf{\Theta}_1^{dl}\mathbf{H}_1 + \mathbf{H}_2$. In the DL energy harvesting phase, the transmitted signal from the HAP can be expressed as $\mathbf{x} = \sum_{k=1}^K \mathbf{w}_k s_k^{dl}$, where s_k^{dl} denotes the energy signal, and $s_k^{dl} \sim \mathcal{CN}(0,1)$, $\mathbf{w}_k \in \mathbb{C}^{M\times 1}$. Moreover, the transmit power of the HAP in DL is represented by $\mathbb{E}\left\{\|\mathbf{x}\|^2\right\} = \sum_{k=1}^K \|\mathbf{w}_k\|^2$, which cannot exceed the maximum transmit power of HAP $P_{\max}$. Hence, we have

$$\sum_{k=1}^K \|\mathbf{w}_k\|^2 \leq P_{\max}. \tag{7}$$

In the DL, the energy transmitted by the HAP can be written as

$$E_{EH} = (T - t_c)\sum_{k=1}^K \|\mathbf{w}_k\|^2. \tag{8}$$

As a PS protocol is employed in the double zeRIS-aided energy harvesting model, thus, the received power at the RIS 1 and RIS 2 are

$$P_{ris,1}^{in} = \sum_{k=1}^K \mathrm{tr}\left(\mathbf{w}_k^H \mathbf{G}_1 \mathbf{w}_k\right), \tag{9}$$

and

$$P_{ris,2}^{in} = \sum_{k=1}^K \mathrm{tr}\left(\mathbf{w}_k^H \mathbf{G}_2 \mathbf{w}_k\right), \tag{10}$$

This article has been accepted for publication in a future issue of this journal, but has not been fully edited. Content may change prior to final publication.
Citation information: DOI: 10.1109/TWC.2025.3581097, IEEE Transactions on Wireless Communications

respectively, where $\mathbf{G}_1 = E\left\{\mathbf{H}_1^H\mathbf{H}_1\right\}$, and $\mathbf{G}_2 = E\left\{\widehat{\mathbf{H}}_2^H\widehat{\mathbf{H}}_2\right\}$. Moreover, the reflected power of RIS 1 and RIS 2 are given by

$$P_{ris,1}^{out} = \sum_{k=1}^{K} \mathrm{tr}\left(\mathbf{w}_k^H\mathbf{H}_1^H(\mathbf{\Theta}_1^{dl})^H\mathbf{\Theta}_1^{dl}\mathbf{H}_1\mathbf{w}_k\right), \quad (11)$$

and

$$P_{ris,2}^{out} = \sum_{k=1}^{K} \mathrm{tr}\left(\mathbf{w}_k^H\widehat{\mathbf{H}}_2^H(\mathbf{\Theta}_2^{dl})^H\mathbf{\Theta}_2^{dl}\widehat{\mathbf{H}}_2\mathbf{w}_k\right). \quad (12)$$

Consequently, the split power of the received signal at the r-th RIS is determined as $P_{ris,r} = P_{ris,r}^{in} - P_{ris,r}^{out}$ [16], [47], i.e.,

$$P_{ris,1} = \sum_{k=1}^{K} \mathrm{tr}\left(\mathbf{w}_k^H\mathbf{H}_1^H\left(\mathbf{I} - (\mathbf{\Theta}_1^{dl})^H\mathbf{\Theta}_1^{dl}\right)\mathbf{H}_1\mathbf{w}_k\right), \quad (13)$$

and

$$P_{ris,2} = \sum_{k=1}^{K} \mathrm{tr}\left(\mathbf{w}_k^H\widehat{\mathbf{H}}_2^H\left(\mathbf{I} - (\mathbf{\Theta}_2^{dl})^H\mathbf{\Theta}_2^{dl}\right)\widehat{\mathbf{H}}_2\mathbf{w}_k\right). \quad (14)$$

Regarding energy harvesting, we adopt a broadly used non-linear model based on logistic functions [48], which is modeled as

$$\Xi(x) = \frac{\delta_{\max}}{X\left(1+\exp\left(-a_{\mathrm{eh}}\left(x-b_{\mathrm{eh}}\right)\right)\right)} - Y, \quad (15)$$

where x denotes the received power, $\delta_{\max}$ represents the maximum power harvested when the circuit reaches saturation, a_{eh} and b_{eh} are parameters specific to the circuit's design. Furthermore, X is defined as $\frac{\exp(a_{\mathrm{eh}}b_{\mathrm{eh}})}{1+\exp(a_{\mathrm{eh}}b_{\mathrm{eh}})}$, and Y is calculated as $\frac{\delta_{\max}}{\exp(a_{\mathrm{eh}}b_{\mathrm{eh}})}$. Additionally, the inverse function of $\Xi(x)$ is defined by [47]

$$\Xi^{-1}(x) = b_{\mathrm{eh}} - \frac{1}{a_{\mathrm{eh}}}\ln\left(\frac{\delta_{\max}}{(x+Y)X} - 1\right). \quad (16)$$

By doing so, the harvested energy at RIS 1 and RIS 2 can be expressed as

$$E_{ris,1} = (T-t_c)\,\Xi(P_{ris,1}), \quad (17)$$

and

$$E_{ris,2} = (T-t_c)\,\Xi(P_{ris,2}), \quad (18)$$

respectively. Given that the circuit power consumption for each element in each RIS is denoted by μ, thus, the aggregate power requirement for each RIS is expressed as $N\mu$ [49]. Consequently, the harvested power for each RIS must be no less than $N\mu$. Assuming that all harvested energy stored in the energy reservoir is used to power the RIS circuits, the following constraints are formulated.

$$TN\mu \leqslant E_{ris,1}, \quad (19)$$
$$TN\mu \leqslant E_{ris,2}. \quad (20)$$

It is important to note that the positions of the HAP, RIS 1, and RIS 2 are usually deployed in advance, so $\mathbf{G}_1$ and $\mathbf{G}_2$ are typically predetermined in the deployment phase. As the antenna noise power, is negligible compared to the harvesting power [50], by neglecting the noise, the power of the received signal at the kth ZED can be given by

$$P_k = \sum_{i=1}^{K} \mathrm{tr}\left(\mathbf{w}_i^H\mathbf{\Phi}_k\mathbf{w}_i\right), \forall k. \quad (21)$$

The harvested energy at the k-th ZED is expressed by

$$E_k = (T-t_c)\,\Xi(P_k), \forall k. \quad (22)$$

C. Computation Offloading

1) Communication Model: In the second sub-block of duration t_c, ZEDs use the harvested energy to offload tasks to the server at the HAP [30], [51], [52]. Furthermore, the time required for the ZEDs to download the results is neglected [30]. In the UL model, ZEDs utilize time division multiple access (TDMA) technology for communication with the HAP [39]. The transmission signal from the k-th ZED is expressed as

$$x_k = \sqrt{p_k}s_k^{ul}, \forall k, \quad (23)$$

where s_k^{ul} symbolizes the information signal transmitted by the k-th ZED, and $s_k^{ul} \sim \mathcal{CN}(0,1), \forall k$. Additionally, p_k represents the transmit power of the k-th ZED. Thus, the signal received at the HAP can be mathematically represented as

$$\mathbf{y} = \sum_{k=1}^{K} \mathbf{\Omega}_k^{ul}\sqrt{p_k}s_k^{ul} + \mathbf{n_a}, \quad (24)$$

where $\mathbf{n_a} \sim \mathcal{CN}\left(0,\sigma_n^2\mathbf{I}_N\right)$. Let $\mathbf{v}_k \in \mathbb{C}^{M\times 1}$ be the beamforming vector for decoding the information signal s_k^{ul} transmitted by the k-th ZED. Then we have

$$\mathrm{SINR}_k^{ul} = \frac{p_k\left|\left(\mathbf{\Omega}_k^{ul}\right)^H\mathbf{v}_k\right|^2}{\sigma_n^2\left\|\mathbf{v}_k\right\|^2}, \forall k. \quad (25)$$

Consequently, the achievable offloading rate for the k-th ZED is determined by

$$R_k^{ul}(p_k,\mathbf{v}_k,\mathbf{\Theta}_r^{ul}) = B\log_2\left(1+\frac{p_k\mathbf{v}_k^H\mathbf{\Psi}_k\mathbf{v}_k}{\sigma_n^2\mathbf{v}_k^H\mathbf{v}_k}\right), \forall k, \quad (26)$$

where B is the bandwidth.

2) Computing Model: In this model, the k-th edge ZED offloads a fixed task ℓ_k to the HAP for processing via MEC. For the computation offloading, the offloading time of the k-th ZED is

$$t_k^{off} = \frac{\ell_k}{R_k^{ul}}, \forall k. \quad (27)$$

Since the computing time and the time required for the HAP to transmit back the processed tasks can be quite small, we assume that they are negligible [42]. Thus, we have

$$\sum_{k=1}^{K} t_k^{off} \leqslant t_c, \quad (28)$$

should be satisfied. The offloading energy consumption at the k-th ZED is given by

$$E_k^{off} = p_k\frac{\ell_k}{R_k^{ul}}, \forall k. \quad (29)$$

This article has been accepted for publication in a future issue of this journal, but has not been fully edited. Content may change prior to final publication.
Citation information: DOI: 10.1109/TWC.2025.3581097, IEEE Transactions on Wireless Communications

As the harvested energy by the k-th ZED should cover the energy consumption of UL communication, thus, we have

$$E_k^{off} \leqslant E_k, \forall k. \tag{30}$$

We assume that the energy consumption of the HAP-MEC server follows a linear model [33], and can be given as

$$E_{MEC} = \rho \sum_{k=1}^{K} \ell_k, \tag{31}$$

where ρ denotes the HAP's energy consumption to process each unit of workload.

III. Problem Formulation and Energy Minimization Design

In this section, an energy minimization problem is formulated, including the energy consumed for transmitting the energy signal and computing the workloads. Then, an iterative solution is designed by applying a series of mathematical methods.

A. Problem Formulation

We jointly optimize the DL energy beamforming matrix at the HAP $\mathbf{W}_{dl} \triangleq [\mathbf{w}_1, \cdots, \mathbf{w}_K] \in \mathbb{C}^{M\times K}$ and the UL receive beamforming matrix $\mathbf{V} \triangleq [\mathbf{v}_1, \cdots, \mathbf{v}_K] \in \mathbb{C}^{M\times K}$ at the HAP, the energy reflection coefficient matrices for zeRISs $\mathbf{\Theta}_r^{dl}$, $r \in \{1,2\}$, the information reflection coefficient matrices for zeRISs $\mathbf{\Theta}_r^{ul}$, $r \in \{1,2\}$, the transmit powers for the ZEDs $\mathbf{p} \triangleq \{p_1, \cdots, p_K\}$, and the time allocation t_c. The optimization problem can be formulated as follows:

$$\begin{aligned}
\min_{t_c, \mathbf{W}_{dl}, \mathbf{V}, \mathbf{\Theta}_r^{dl}, \mathbf{p}, \mathbf{\Theta}_r^{ul}} & \sum_{k=1}^{K} \left((T - t_c) \left\| \mathbf{w}_k \right\|^2 + \rho \ell_k \right) \qquad \text{(P1)} \\
\text{s.t. } & C1: \left| \beta_{r,n}^{ul/dl} e^{j\theta_{r,n}^{ul/dl}} \right| \leqslant 1, \forall n, r \in \{1,2\}, \\
& C2: \sum_{k=1}^{K} \left\| \mathbf{w}_k \right\|^2 \leq P_{\max}, \\
& C3: TN\mu \leqslant E_{ris,r}, r \in \{1,2\}, \\
& C4: E_k^{off} \leqslant E_k, \forall k, \\
& C5: \sum_{k=1}^{K} t_k^{off} \leqslant t_c, \\
& C6: p_k \geqslant 0, \forall k, \\
& C7: t_c \in (0, T).
\end{aligned}$$

In (P1), $C1$ is the unit-modulus constraint on the reflection coefficients of the RISs in the DL and UL, respectively. $C3$ means that the energy harvested by each RIS should cover the corresponding circuit power consumption. Constraint $C4$ implies that the energy harvested by each ZED should cover the related circuit power consumption and computing offloading power consumption, and $C5$ is the constraint on the duration of UL task offloading.

Compared to using a single RIS, the existence of cascaded zeRISs with dual-reflection links and a nonlinear harvesting model makes problem (P1) a non-convex optimization challenge. In this scenario, the HAP beamforming, the reflection coefficients of the zeRISs, the transmit powers for the ZEDs, and the time allocation are strongly coupled. To address these challenges, we use the AO method to decouple the original problem into seven sub-problems. In each iteration, while keeping other optimization variables fixed, we iteratively optimize one variable until the value of the objective function converges.

B. Problem Transformation

Firstly, by integrating (16) with (29), the original constraint $C4$ is transformed as:

$$C8: \sum_{i=1}^{K} \mathrm{tr}\left(\mathbf{\Phi}_k \mathbf{W}_i\right) \geqslant \Xi^{-1}\left(\frac{p_k \frac{\ell_k}{R_k^{ul}}}{T - t_c}\right), \forall k,$$

where $\mathbf{W}_i = \mathbf{w}_i \mathbf{w}_i^H \succeq 0$, and $\mathrm{rank}\left(\mathbf{W}_i\right) = 1$ should be satisfied.

Further, by letting $\mathbf{V}_k = \mathbf{v}_k \mathbf{v}_k^H \succeq 0$, and $\mathrm{rank}\left(\mathbf{V}_k\right) = 1$, the initial problem (P1) can be reformulated as problem (P2)

$$\begin{aligned}
\min_{t_c, \mathbf{W}_k, \mathbf{V}_k, \mathbf{\Theta}_r^{dl}, \mathbf{p}, \mathbf{\Theta}_r^{ul}} & \sum_{k=1}^{K} \left[(T - t_c) \,\mathrm{tr}(\mathbf{W}_k) + \rho \ell_k \right] \qquad \text{(P2)} \\
\text{s.t. } & C1, C6 - C8, \\
& C9: \sum_{k=1}^{K} \mathrm{tr}(\mathbf{W}_k) \leq P_{\max}, \\
& C10: \mathbf{W}_k \succeq 0, \mathrm{rank}\left(\mathbf{W}_k\right) = 1, \forall k, \\
& C11: \mathbf{V}_k \succeq 0, \mathrm{rank}\left(\mathbf{V}_k\right) = 1, \forall k, \\
& C12: \sum_{k=1}^{K} \mathrm{tr}\left(\mathbf{H}_1^H \left(\mathbf{I} - (\mathbf{\Theta}_1^{dl})^H \mathbf{\Theta}_1^{dl}\right) \mathbf{H}_1 \mathbf{W}_k\right) \\
& \qquad \geqslant \Xi^{-1}\left(\frac{T}{T - t_c} N\mu\right), \\
& C13: \sum_{k=1}^{K} \mathrm{tr}\left(\widehat{\mathbf{H}}_2^H \left(\mathbf{I} - (\mathbf{\Theta}_2^{dl})^H \mathbf{\Theta}_2^{dl}\right) \widehat{\mathbf{H}}_2 \mathbf{W}_k\right) \\
& \qquad \geqslant \Xi^{-1}\left(\frac{T}{T - t_c} N\mu\right).
\end{aligned}$$

To solve Problem (P2), the AO method is adopted to solve the variables in the UL phase and DL phase in an iterative manner.

C. UL Computing Phase Optimization

In this subsection, we aim to optimize the computing phase design, with a fixed t_c, $\mathbf{W}_{dl}$, and $\mathbf{\Theta}_r^{dl}$. By doing so, we simplify Problem (P1) as

$$\begin{aligned}
\min_{\mathbf{V}, \mathbf{p}, \mathbf{\Theta}_r^{ul}} & \rho \sum_{k=1}^{K} \ell_k \qquad \text{(P3)} \\
\text{s.t. } & C4 - C6, C11, \\
& C14: \left| \beta_{r,n}^{ul} e^{j\theta_{r,n}^{ul}} \right| \leqslant 1, \forall n, r \in \{1,2\}.
\end{aligned}$$

In this paper, a linear receive beamforming vector $\mathbf{v}_k^* \in \mathbb{C}^{M\times 1}$ is deployed at the HAP [40]. We assume that the HAP employs a Maximum Ratio Combining (MRC) strategy

This article has been accepted for publication in a future issue of this journal, but has not been fully edited. Content may change prior to final publication.
Citation information: DOI: 10.1109/TWC.2025.3581097, IEEE Transactions on Wireless Communications

to decode the k-th ZED's information, and the receiving beamforming vector of the HAP is given as

$$\mathbf{v}_k^* = \frac{\mathbf{\Omega}_k^{ul}}{\left\|\mathbf{\Omega}_k^{ul}\right\|}, \forall k. \tag{32}$$

1) Optimizing the Information Reflection Coefficient Matrices for zeRISs at UL Phase: Since the objective function in problem (P3) is independent of the optimization variable $\mathbf{\Theta}_r^{ul}$, we instead maximize R_k^{ul} to ensure that related latency and energy constraints can be well satisfied. This is equivalent to maximizing the zeRIS-assisted UL channel gain from the k-th ZED to the HAP by optimizing $\mathbf{\Theta}_r^{ul}$. Therefore, given the transmit power vector $\mathbf{p}$, we solve the information reflection coefficient matrices for zeRISs as follows:

$$\begin{aligned} \max_{\mathbf{\Theta}_r^{ul}} \ & \left\|\mathbf{\Omega}_k^{ul}\right\|^2 \\ \text{s.t. } & C14. \end{aligned} \tag{P3.1}$$

By denoting $\bar{\mathbf{H}}_k \triangleq [\bar{\mathbf{h}}_{k,1}, \cdots, \bar{\mathbf{h}}_{k,N}] = \mathbf{H}_{1,2}^H \mathrm{diag}(\mathbf{h}_{2,k})$. It should be noted that

$$\begin{aligned} \left\|\mathbf{\Omega}_k^{ul}\right\|^2 &= \left\|\mathbf{\Upsilon}_k^{ul}\boldsymbol{\theta}_2^{ul} + \boldsymbol{\eta}_k^{ul}\right\|^2 \\ &= (\mathbf{\Upsilon}_k^{ul}\boldsymbol{\theta}_2^{ul} + \boldsymbol{\eta}_k^{ul})^H(\mathbf{\Upsilon}_k^{ul}\boldsymbol{\theta}_2^{ul} + \boldsymbol{\eta}_k^{ul}) \\ &= (\boldsymbol{\theta}_2^{ul})^H(\mathbf{\Upsilon}_k^{ul})^H\mathbf{\Upsilon}_k^{ul}\boldsymbol{\theta}_2^{ul} + (\boldsymbol{\theta}_2^{ul})^H(\mathbf{\Upsilon}_k^{ul})^H\boldsymbol{\eta}_k^{ul} \\ &\quad + (\boldsymbol{\eta}_k^{ul})^H\mathbf{\Upsilon}_k^{ul}\boldsymbol{\theta}_2^{ul} + (\boldsymbol{\eta}_k^{ul})^H\boldsymbol{\eta}_k^{ul}, \end{aligned} \tag{33}$$

where

$$\mathbf{\Upsilon}_k^{ul} = \mathbf{H}_1^H \sum_{n=1}^{N} \mathrm{diag}(\bar{\mathbf{h}}_{k,n})\theta_{1,n}^{ul} + \mathbf{H}_2^H \mathrm{diag}(\mathbf{h}_{2,k}), \tag{34}$$

$$\boldsymbol{\eta}_k^{ul} = \mathbf{H}_1^H \mathrm{diag}(\mathbf{h}_{1,k})\boldsymbol{\theta}_1^{ul}. \tag{35}$$

Next, by introducing an auxiliary variable l such that $\mathbf{Z}^{ul} = \bar{\boldsymbol{\theta}}_2^{ul}\left(\bar{\boldsymbol{\theta}}_2^{ul}\right)^H$, where $\bar{\boldsymbol{\theta}}_2^{ul} = \left[\boldsymbol{\theta}_2^{ul}, l\right]^T$, we have $\left\|\mathbf{\Omega}_k^{ul}\right\|^2 = \mathrm{tr}\left(\mathbf{\Upsilon}_k^{ul\prime}\mathbf{Z}^{ul}\right) + \left\|\boldsymbol{\eta}_k^{ul}\right\|^2$, where

$$\mathbf{\Upsilon}_k^{ul\prime} = \begin{bmatrix} (\mathbf{\Upsilon}_k^{ul})^H\mathbf{\Upsilon}_k^{ul} & (\boldsymbol{\eta}_k^{ul})^H\mathbf{\Upsilon}_k^{ul} \\ (\mathbf{\Upsilon}_k^{ul})^H\boldsymbol{\eta}_k^{ul} & 0 \end{bmatrix}. \tag{36}$$

Since $\mathbf{Z}^{ul} = \bar{\boldsymbol{\theta}}_2^{ul}\left(\bar{\boldsymbol{\theta}}_2^{ul}\right)^H$, the constraints of $\mathbf{Z}^{ul} \succeq 0$ and $\mathrm{rank}\left(\mathbf{Z}^{ul}\right) = 1$ should be satisfied. Based on the above, given the information reflection coefficient matrix $\mathbf{\Theta}_1^{ul}$, we relax the rank-one constraint and subsequently reformulate the sub-problem for the information reflection coefficient matrix of zeRIS 2 during the UL transmission as follows

$$\begin{aligned} \max_{\mathbf{Z}^{ul}} \ & \mathrm{tr}\left(\mathbf{\Upsilon}_k^{ul\prime}\mathbf{Z}^{ul}\right) + \left\|\boldsymbol{\eta}_k^{ul}\right\|^2 \\ \text{s.t. } & C15: \mathbf{Z}^{ul} \succeq 0, \\ & C16: \mathbf{Z}_{n,n}^{ul} \leqslant 1, \forall n. \end{aligned} \tag{P3.1.1}$$

Let $\mathbf{U}_k^{ul} = \sum_{n=1}^{N} \mathbf{H}_2^H \mathrm{diag}(\bar{\mathbf{h}}_{k,n})\theta_{2,n}^{ul} + \mathbf{H}_1^H \mathrm{diag}(\mathbf{h}_{1,k})$, and $\boldsymbol{\lambda}_k^{ul} = \mathbf{H}_2^H \mathrm{diag}(\mathbf{h}_{2,k})\boldsymbol{\theta}_2^{ul}$. Next, with the given $\mathbf{\Theta}_2^{ul}$, we then follow similar procedures with problem (P3.1.1) and reformulate the sub-problem of the reflection coefficient matrix for zeRIS 1 during UL as

$$\begin{aligned} \max_{\mathbf{Q}^{ul}} \ & \mathrm{tr}\left(\mathbf{U}_k^{ul\prime}\mathbf{Q}^{ul}\right) + \left\|\boldsymbol{\lambda}_k^{ul}\right\|^2 \\ \text{s.t. } & C17: \mathbf{Q}^{ul} \succeq 0, \\ & C18: \mathbf{Q}_{n,n}^{ul} \leqslant 1, \forall n, \end{aligned} \tag{P3.1.2}$$

where

$$\mathbf{U}_k^{ul\prime} = \begin{bmatrix} (\mathbf{U}_k^{ul})^H\mathbf{U}_k^{ul} & (\boldsymbol{\lambda}_k^{ul})^H\mathbf{U}_k^{ul} \\ (\mathbf{U}_k^{ul})^H\boldsymbol{\lambda}_k^{ul} & 0 \end{bmatrix}, \tag{37}$$

$\mathbf{Q}^{ul} = \bar{\boldsymbol{\theta}}_1^{ul}\left(\bar{\boldsymbol{\theta}}_1^{ul}\right)^H$, and $\bar{\boldsymbol{\theta}}_1^{ul} = \begin{bmatrix} \boldsymbol{\theta}_1^{ul} \\ l \end{bmatrix}$.

As such, the problem (P3.1.1) and (P3.1.2) are convex SDP problems that can be addressed using the CVX toolbox [53]. Then we employ the Gaussian randomization method to construct a suboptimal rank-one solution, following a process similar to [47], which is omitted here.

2) Design of the Transmit Powers for the ZEDs : Given $\mathbf{\Theta}_1^{ul}$ and $\mathbf{\Theta}_2^{ul}$ to problem (P3.1) and the receiving beamforming vector of HAP $\mathbf{v}_k^*$, $R_k^{ul}(p_k, \mathbf{v}_k^*, \mathbf{\Theta}_r^{ul*})$ only depends on the transmit power p_k. Then, the achievable offloading rate for the k-th ZED is determined by

$$R_k^{ul} = B\log_2\left(1 + \frac{p_k\left\|\mathbf{\Omega}_k^{ul*}\right\|^2}{\sigma_n^2}\right), \forall k. \tag{38}$$

By substituting (27) into C4 and C5, the following constraints can be obtained:

$$C19: R_k^{ul}E_k \geqslant p_k\ell_k, \forall k,$$

$$C20: \sum_{k=1}^{K}\frac{\ell_k}{R_k^{ul}} \leqslant t_c.$$

Subsequently, we optimize p_k by solving the sub-problem (P3.2) :

$$\begin{aligned} \text{find} \quad & p_k \\ \text{s.t. } & C6, C19, C20. \end{aligned} \tag{P3.2}$$

Since all the constraints are convex, Problem (P3.2) is a convex optimization problem, and it can be solved by CVX [53]. Algorithm 1 summarizes the optimization of the beamforming of the HAP, the reflection coefficient matrices for zeRISs, and the transmit power allocation for the ZEDs during UL.

D. DL Beamforming Optimization

Given the time allocation t_c and the settings of $\mathbf{p}, \mathbf{\Theta}_r^{ul}$. Consequently, the problem initially presented in (P1) can be reformulated as problem (P4):

$$\begin{aligned} \min_{\mathbf{W}_k, \mathbf{\Theta}_r^{dl}} \ & \sum_{k=1}^{K}(T - t_c)\,\mathrm{tr}(\mathbf{W}_k), \\ \text{s.t. } & C8 - C10, C12, C13, \\ & C21: \left|\beta_{r,n}^{dl}e^{j\theta_{r,n}^{dl}}\right| \leqslant 1, \forall n, r \in \{1,2\}. \end{aligned} \tag{P4}$$

We note that the optimization problem (P4) remains non-convex; due to the optimization variable $\mathbf{W}_k$ being coupled with $\mathbf{\Theta}_r^{dl}$ in constraints C8, C12, C13. Thus, we employ AO and SDP techniques to iteratively optimize one of the two variables while keeping the other fixed, as detailed below.

This article has been accepted for publication in a future issue of this journal, but has not been fully edited. Content may change prior to final publication.
Citation information: DOI: 10.1109/TWC.2025.3581097, IEEE Transactions on Wireless Communications

Algorithm 1 AO Algorithm for Solving Problem (P3)

Input: Set $\{t_c^0, \mathbf{W}_{dl}^0, \mathbf{\Theta}_r^{dl,0}\}$, B, N, M, K, μ, ℓ_k, ρ, convergence threshold ϵ, and iteration index t=0.

1: Obtain the optimal UL receive beamforming matrix at the HAP $\mathbf{V}^*$ by (32).
2: **repeat**
3: Given $\{\mathbf{p}^t, \mathbf{\Theta}_1^{ul,t}\}$, obtain the suboptimal reflection coefficient matrix for zeRIS 2, $\mathbf{\Theta}_2^{ul,t+1}$ by solving problem (P3.1.1).
4: Given $\{\mathbf{p}^t, \mathbf{\Theta}_2^{ul,t+1}\}$, obtain the suboptimal reflection coefficient matrix for zeRIS 1, $\mathbf{\Theta}_1^{ul,t+1}$ by solving problem (P3.1.2).
5: Given $\{\mathbf{\Theta}_1^{ul,t+1}, \mathbf{\Theta}_2^{ul,t+1}\}$, obtain the optimal transmit power $\mathbf{p}^{t+1}$ by solving problem (P3.2) .
6: Update the iterative number $t = t + 1$.
7: **until** Convergence.

Output: the HAP's UL receive beamforming $\mathbf{V}^*$, the transmit powers of the ZEDs $\mathbf{p}^*$, the information reflection coefficient matrices for zeRISs $\mathbf{\Theta}_r^{ul*}$.

1) Optimization of Energy Beamforming at the HAP: Fixed $\mathbf{\Theta}_r^{dl}$, the problem (P4) is transformed into the problem (P4.1), which is given by

$$\min_{\mathbf{W}_k} \sum_{k=1}^{K} (T - t_c)\,\mathrm{tr}(\mathbf{W}_k) \quad \text{(P4.1)}$$
$$\text{s.t. } C8 - C10, C12, C13.$$

By relaxing the rank-one constraint, $\mathrm{Rank}(\mathbf{W}_k) \leqslant 1$, the problem (P4.1) is reformulated as an SDP problem and can be solved by CVX [53]. In this paper, we employ the Gaussian randomization technique to construct a suboptimal rank-one solution, following the methodology outlined in [47].

2) Optimizing the Energy Reflection Coefficient Matrices for the zeRISs at DL Phase: In the following, we jointly optimize the two parameters: the reflection amplitudes and the reflection coefficients of the RIS, as discussed in [47]. The optimal solution to problem (P4.1) is denoted by $\mathbf{W}^*$. Subsequently, we alternately solve for the reflection coefficient matrices of zeRIS 2 and zeRIS 1. Given $\mathbf{\Theta}_1^{dl}$, we solve the energy reflection coefficient matrix for RIS 2 as follows:

$$\text{find } \mathbf{\Theta}_2^{dl} \quad \text{(P4.2)}$$
$$\text{s.t. } C8, C13,$$
$$C22: \left|\beta_{2,n}^{dl} e^{j\theta_{2,n}^{dl}}\right| \leqslant 1, \forall n,$$

The sub-problem remains non-convex due to the coupling of variables in the constraints. To make it tractable, we set $\mathcal{G}_{2,k}^{'} = \mathrm{diag}(\bar{\mathbf{H}}_2 \mathbf{w}_k \mathbf{w}_k^H \bar{\mathbf{H}}_2^H, 0)$, $\bar{\boldsymbol{\theta}}_2^{dl} = [\boldsymbol{\theta}_2^{dl}, l]$, and $\mathbf{Z}^{dl} = \left(\bar{\boldsymbol{\theta}}_2^{dl}\right)^H \bar{\boldsymbol{\theta}}_2^{dl}$, thus, the constraints C13 can be rewritten as

$$C23: \sum_{k=1}^{K} \mathrm{tr}\left(\mathcal{G}_{2,k}^{'}\right) - \sum_{k=1}^{K} \mathrm{tr}\left(\mathcal{G}_{2,k}^{'} \mathbf{Z}^{dl}\right) \geqslant \Xi^{-1}\left(\frac{T}{T - t_c} N\mu\right),$$

To proceed, we let

$$\bar{\mathbf{D}}_k \triangleq [\bar{\mathbf{d}}_{k,1}, \cdots, \bar{\mathbf{d}}_{k,N}] = \mathrm{diag}(\mathbf{h}_{2,k}^H)\mathbf{H}_{1,2}, \quad (39)$$

$$\boldsymbol{q}_{k,i}^{dl} = \left(\sum_{n=1}^{N} \theta_{1,n}^{dl} \mathrm{diag}(\bar{\mathbf{d}}_{k,n})\mathbf{H}_1 + \mathrm{diag}(\mathbf{h}_{2,k}^H)\mathbf{H}_2\right)\mathbf{w}_i, \quad (40)$$

$$\eta_{k,i}^{dl} = \boldsymbol{\theta}_1^{dl} \mathrm{diag}(\mathbf{h}_{1,k}^H)\mathbf{H}_1 \mathbf{w}_i. \quad (41)$$

We note that the left-hand side of constraint C8 can be expressed as

$$\mathrm{tr}\left(\mathbf{\Phi}_k \mathbf{W}_i\right) = \left|\boldsymbol{\theta}_2^{dl} \boldsymbol{q}_{k,i}^{dl} + \eta_{k,i}^{dl}\right|^2, \quad (42)$$

then we transform $\left|\boldsymbol{\theta}_2^{dl} \boldsymbol{q}_{k,i}^{dl} + \eta_{k,i}^{dl}\right|^2$ as $\bar{\boldsymbol{\theta}}_2^{dl} \boldsymbol{\Upsilon}_{k,i}^{dl} \left(\bar{\boldsymbol{\theta}}_2^{dl}\right)^H + \left|\eta_{k,i}^{dl}\right|^2$, where $\bar{\boldsymbol{\theta}}_2^{dl} = \left[\boldsymbol{\theta}_2^{dl}, l\right]$,

$$\boldsymbol{\Upsilon}_{k,i}^{dl} = \begin{bmatrix} \boldsymbol{q}_{k,i}^{dl}(\boldsymbol{q}_{k,i}^{dl})^H & \boldsymbol{q}_{k,i}^{dl}(\eta_{k,i}^{dl})^H \\ \eta_{k,i}^{dl}(\boldsymbol{q}_{k,i}^{dl})^H & 0 \end{bmatrix}. \quad (43)$$

Since $\bar{\boldsymbol{\theta}}_2^{dl} \boldsymbol{\Upsilon}_{k,i}^{dl} \left(\bar{\boldsymbol{\theta}}_2^{dl}\right)^H = \mathrm{tr}\left(\boldsymbol{\Upsilon}_{k,i}^{dl} \left(\bar{\boldsymbol{\theta}}_2^{dl}\right)^H \bar{\boldsymbol{\theta}}_2^{dl}\right)$, we have $\bar{\boldsymbol{\theta}}_2^{dl} \boldsymbol{\Upsilon}_{k,i}^{dl} \left(\bar{\boldsymbol{\theta}}_2^{dl}\right)^H = \mathrm{tr}\left(\boldsymbol{\Upsilon}_{k,i}^{dl} \mathbf{Z}^{dl}\right)$. Based on the above, the constraints C8 in problem (P4.2) can be rewritten as

$$C24: \sum_{i=1}^{K} \mathrm{tr}\left(\boldsymbol{\Upsilon}_{k,i}^{dl} \mathbf{Z}^{dl}\right) + \sum_{i=1}^{K} \left|\eta_{k,i}^{dl}\right|^2 \geqslant \Xi^{-1}\left(\frac{p_k \frac{\ell_k}{R_k^{ul}}}{(T - t_c)}\right), \forall k.$$

Furthermore, due to $\mathbf{Z}^{dl} = \left(\bar{\boldsymbol{\theta}}_2^{dl}\right)^H \bar{\boldsymbol{\theta}}_2^{dl}$, the constraints of $\mathbf{Z}^{dl} \succeq 0$ and $\mathrm{rank}\left(\mathbf{Z}^{dl}\right) = 1$ should be satisfied. By relaxing the rank-one constraint, we solve the reflection coefficient matrix of zeRIS 2 as follows

$$\text{find } \mathbf{Z}^{dl} \quad \text{(P4.3)}$$
$$\text{s.t. } C23, C24,$$
$$C25: \mathbf{Z}^{dl} \succeq 0,$$
$$C26: \mathbf{Z}_{n,n}^{dl} \leqslant 1, \forall n.$$

Next, with the given $\mathbf{\Theta}_2^{dl}$, the energy reflection coefficient matrix for zeRIS 1 can be derived by

$$\text{find } \mathbf{\Theta}_1^{dl} \quad \text{(P4.4)}$$
$$\text{s.t. } C8, C12,$$
$$C27: \left|\beta_{1,n}^{dl} e^{j\theta_{1,n}^{dl}}\right| \leqslant 1, \forall n.$$

The sub-problem remains non-convex due to variable coupling in the constraints. To solve this, we adopt a similar approach as in (P4.2)-(P4.3) and first set $\mathbf{R}_{1,k}^{'} = \mathrm{diag}(\mathbf{H}_1 \mathbf{w}_k \mathbf{w}_k^H \mathbf{H}_1^H, 0)$, $\bar{\boldsymbol{\theta}}_1^{dl} = \left[\boldsymbol{\theta}_1^{dl}, l\right]$, and $\mathbf{Q}^{dl} = \left(\bar{\boldsymbol{\theta}}_1^{dl}\right)^H \bar{\boldsymbol{\theta}}_1^{dl}$, thus, the constraints C13 can be rewritten as

$$C28: \sum_{k=1}^{K} \mathrm{tr}\left(\mathbf{R}_{1,k}^{'}\right) - \sum_{k=1}^{K} \mathrm{tr}\left(\mathbf{R}_{1,k}^{'} \mathbf{Q}^{dl}\right) \geqslant \Xi^{-1}\left(\frac{T}{T - t_c} N\mu\right).$$

Similarly, by denoting

$$\mathbf{u}_{k,i}^{dl} = \left(\sum_{n=1}^{N} \theta_{2,n}^{dl} \mathrm{diag}(\bar{\mathbf{d}}_{k,n})\mathbf{H}_1 + \mathrm{diag}(\mathbf{h}_{1,k}^H)\mathbf{H}_1\right)\mathbf{w}_i, \quad (44)$$

This article has been accepted for publication in a future issue of this journal, but has not been fully edited. Content may change prior to final publication.
Citation information: DOI: 10.1109/TWC.2025.3581097, IEEE Transactions on Wireless Communications

$$\lambda_{k,i}^{dl} = \boldsymbol{\theta}_2^{dl} \mathrm{diag}(\mathbf{h}_{2,k}^H)\mathbf{H}_2\mathbf{w}_i. \tag{45}$$

The left-hand side of C8 can be expressed as

$$\mathrm{tr}\left(\boldsymbol{\Phi}_k \mathbf{W}_i\right) = \left|\boldsymbol{\theta}_1^{dl}\mathbf{u}_{k,i}^{dl} + \lambda_{k,i}^{dl}\right|^2, \tag{46}$$

then we transform $\left|\boldsymbol{\theta}_1^{dl}\mathbf{u}_{k,i}^{dl} + \lambda_{k,i}^{dl}\right|^2$ as $\bar{\boldsymbol{\theta}}_1^{dl}\mathbf{U}_{k,i}^{dl}\left(\bar{\boldsymbol{\theta}}_1^{dl}\right)^H + \left|\lambda_{k,i}^{dl}\right|^2$, where

$$\mathbf{U}_{k,i}^{dl} = \begin{bmatrix} \mathbf{u}_{k,i}^{dl}(\mathbf{u}_{k,i}^{dl})^H & \mathbf{u}_{k,i}^{dl}(\lambda_{k,i}^{dl})^H \\ \lambda_{k,i}^{dl}(\mathbf{u}_{k,i}^{dl})^H & 0 \end{bmatrix}. \tag{47}$$

Thus, the constraints C8 in problem (P4.4) can be rewritten as

$$C29: \sum_{i=1}^{K} \mathrm{tr}\left(\mathbf{U}_{k,i}^{dl}\mathbf{Q}^{dl}\right) + \sum_{i=1}^{K}\left|\lambda_{k,i}^{dl}\right|^2 \geqslant \Xi^{-1}\left(\frac{p_k \frac{\ell_k}{R_k^{ul}}}{(T-t_c)}\right), \forall k.$$

Therefore, the subproblem concerning the reflection coefficient matrix for zeRIS 1 is subsequently reformulated as follows:

$$\begin{aligned} &\text{find} \quad \mathbf{Q}^{dl} \\ \text{s.t. } &C28, C29, \\ &C30: \mathbf{Q}^{dl} \succeq 0, \\ &C31: \mathbf{Q}_{n,n}^{dl} \leqslant 1, \forall n. \end{aligned} \tag{P4.5}$$

By doing so, the problems (P4.3) and (P4.5) are SDP problems, which can be solved by utilizing the CVX toolbox [53]. Then, a Gaussian randomization method is applied to construct a suboptimal solution that satisfies the rank-one constraint. The process details are similar to those in [47] and are thus omitted for brevity. Therefore, the beamforming design at the HAP and the optimization of the zeRIS reflection coefficient matrices for the DL are presented in Algorithm 2.

Algorithm 2 The Solution for Problem (P4)

Input: Set $\{t_c^0, \mathbf{p}^0, \boldsymbol{\Theta}_r^{ul,0}\}$, $\mathbf{V}^*$, B, N, M, K, μ, ℓ_k, ρ, convergence threshold ϵ, and iteration index $t = 0$.

1: **repeat**
2: Given $\{\boldsymbol{\Theta}_1^{dl,t}, \boldsymbol{\Theta}_2^{dl,t}\}$, obtain $\mathbf{W}_k^{t+1}$ by solving problem (P4.1).
3: Given $\{\boldsymbol{\Theta}_1^{dl,t}, \mathbf{W}_k^{t+1}\}$, obtain the energy reflection coefficient matrix for zeRIS 2, $\boldsymbol{\Theta}_2^{dl,t+1}$ by solving problem (P4.3) and problem (P4.5).
4: Given $\{\boldsymbol{\Theta}_2^{dl,t+1}, \mathbf{W}_k^{t+1}\}$, obtain the energy reflection coefficient matrix for zeRIS 1, $\boldsymbol{\Theta}_1^{dl,t+1}$ by solving problem (P4.5).
5: Update the iterative number $t = t + 1$.
6: **until** Convergence.

Output: the HAP's DL transmit beamforming $\mathbf{W}_{dl}^*$ and the energy reflection coefficient matrices of the zeRISs $\boldsymbol{\Theta}_r^{dl*}$.

E. Time Allocation

For this sub-problem, with the given the beamforming of HAP $\mathbf{W}_{dl}$, $\mathbf{p}$ and the reflection coefficient matrices of the zeRISs $\boldsymbol{\Theta}_r^{dl}, \boldsymbol{\Theta}_r^{ul}$. Problem (P2) can be reformulated as problem (P5) as follows

$$\begin{aligned} \min_{t_c} \ &\sum_{k=1}^{K}\left[(T-t_c)\,\mathrm{tr}(\mathbf{W}_k) + \rho\ell_k\right] \\ \text{s.t. } &C5, C7, \\ &C32: t_c \leqslant T - \frac{TN\mu}{\Xi(P_{ris,r})}, \ r \in \{1,2\}, \\ &C33: t_c \leqslant T - \frac{E_k^{off}}{\Xi(P_k)}, \ \forall k. \end{aligned} \tag{P5}$$

where Constraints C32 and C33 are reformulated based on constraints C3 and C4 in the original problem (P1).

As the objective function decreases monotonically with respect to t_c, t_c is maximized only when at least one equality holds is met, expressed as follows:

$$t_c^* = \min\left(T - \frac{E_k^{off}}{\Xi(P_k)}, T - \frac{TN\mu}{\Xi(P_{ris,r})}\right). \tag{48}$$

F. The Overall Optimization Algorithm in zeRIS-Aided WP-MEC

Algorithm 3 details the proposed method, which iteratively updates the RIS reflection coefficient matrices, HAP beamforming, and optimizes transmit power and time allocation until the change in successive objective values falls below a predefined threshold. The following section presents the analysis of convergence and computational complexity for Algorithm 3.

Algorithm 3 The Overall Optimization Algorithm in zeRIS-Aided WP-MEC

Input: T, Set $\{t_c^0, \mathbf{p}^0, \mathbf{W}_{dl}^0, \boldsymbol{\Theta}_r^{ul,0}, \boldsymbol{\Theta}_r^{dl,0}\}$, B, N, M, K, μ, ℓ_k, ρ, convergence threshold ϵ, and iteration index t=0.

1: **repeat**
2: Given $\{t_c^t, \boldsymbol{\Theta}_r^{dl,t}, \mathbf{W}_{dl}^t\}$, obtain the HAP's UL receive beamforming matrix $\mathbf{V}^{t+1}$, the UL information reflection coefficient matrices for all zeRISs $\boldsymbol{\Theta}_r^{ul,t+1}, \forall r$, and the transmit power allocation for the ZEDs $\mathbf{p}^{t+1}$ following the steps in Algorithm 1.
3: Given $\{t_c^t, \boldsymbol{\Theta}_r^{ul,t}, \mathbf{p}^{t+1}\}$, obtain the HAP's DL transmit beamforming matrix $\mathbf{W}_k^{t+1}$, and the energy reflection coefficients for all zeRISs $\boldsymbol{\Theta}_r^{dl,t+1}, \forall r$, following the steps in Algorithm 2.
4: Obtain t_c^{t+1} according to the problem (P5).
5: Update the iterative number $t = t + 1$.
6: **until** Convergence.

Output: $\mathbf{V}^*$, $\mathbf{p}^*$, $\boldsymbol{\Theta}_r^{ul*}$, $\mathbf{W}_{dl}^*$, $\boldsymbol{\Theta}_r^{dl*}$, t_c^*.

G. The Analysis of Convergence and Computational Complexity

1) Computational Complexity Analysis: Computational complexity of Algorithm 1 is predominantly influenced by

This article has been accepted for publication in a future issue of this journal, but has not been fully edited. Content may change prior to final publication.
Citation information: DOI: 10.1109/TWC.2025.3581097, IEEE Transactions on Wireless Communications

TABLE II: Simulation Parameters

Description	Parameter and Value
System model	$M = 6, N = 200$ $K = 4, T = 1$ s $\mu = 1$ μW
Energy harvesting model	$b_{eh} = 0.24$ $a_{eh} = 150$ $\delta_{\max} = 75$ mW $P_{\max} = 50$ dBm
Communication model	$B = 1$ MHz $\sigma^2 = -174$ dBm
Computing model [33]	$\rho = 5 \times 10^{-8}$ Joule/bit $\ell_k = 20$ Kbit
Convergence criterion	$\epsilon = 0.0001$

the iterative resolution of the problem (P3.1.1), the problem (P3.1.2), and the problem (P3.2). The process of resolving both problems denoted as (P3.1.1) and (P3.1.2) entails a computational complexity quantified by $\mathcal{O}\left(K(N+1)^{3.5}\right)$. The computational complexity of solving problem (P3.2) is $\mathcal{O}\left(K\right)$. Therefore, the computational complexity of Algorithm 1 is $\mathcal{O}\left(KN^{3.5} + 2K(N+1)^{3.5}\right)$. The complexity of Algorithm 2 is primarily governed by the iterative resolution of the SDP problem (P4.1), (P4.2) and problem (P4.5). In each iteration, the problem denoted as (P4.1) is solved employing the interior point method, as referenced in [53]. This approach results in a computational complexity characterized by $\mathcal{O}\left(KN^{3.5}\right)$. Similarly, the computational complexity of Algorithm 2 is $\mathcal{O}\left(KN^{3.5} + 2K(N+1)^{3.5}\right)$. In conclusion, let t represent the number of iterations required for the proposed algorithm to converge. The computational complexity of Algorithm 3 is expressed as $\mathcal{O}\left(t\left(2KN^{3.5} + K + 4K(N+1)^{3.5}\right)\right)$.

2) Convergence Analysis: The proof of the convergence of the proposed Algorithm 3 in zeRIS-empowered WP-MEC is outlined in the following discussion. We define $t_c^t, \mathbf{W}_{dl}^t, \mathbf{V}^t, \mathbf{\Theta}_r^{dl,t}, \mathbf{p}^t, \mathbf{\Theta}_r^{ul,t}$ as the t-th iteration solution of the problem (P4), (P3), and (P5). The objective function is expressed by $E\left(t_c^t, \mathbf{W}_{dl}^t, \mathbf{V}^t, \mathbf{\Theta}_r^{dl,t}, \mathbf{p}^t, \mathbf{\Theta}_r^{ul,t}\right)$

$$E\left(t_c^t, \mathbf{W}_{dl}^t, \mathbf{V}^t, \mathbf{\Theta}_r^{dl,t}, \mathbf{p}^t, \mathbf{\Theta}_r^{ul,t}\right) \tag{49}$$

$$\overset{(a)}{\geq} E\left(t_c^t, \mathbf{W}_{dl}^t, \mathbf{V}^{t+1}, \mathbf{\Theta}_r^{ul,t+1}, \mathbf{p}^t, \mathbf{\Theta}_r^{dl,t}\right) \tag{50}$$

$$\overset{(b)}{\geq} E\left(t_c^t, \mathbf{W}_{dl}^{t+1}, \mathbf{V}^{t+1}, \mathbf{\Theta}_r^{ul,t+1}, \mathbf{p}^{t+1}, \mathbf{\Theta}_r^{dl,t+1}\right) \tag{51}$$

$$\overset{(c)}{\geq} E\left(t_c^{t+1}, \mathbf{W}_{dl}^{t+1}, \mathbf{V}^{t+1}, \mathbf{\Theta}_r^{dl,t+1}, \mathbf{p}^{t+1}, \mathbf{\Theta}_r^{ul,t+1}\right), \tag{52}$$

where (a)-(c) hold due to the update of Algorithm 1-Algorithm 3. The objective function demonstrates a monotonically decreasing behavior across successive iterations of Algorithm 3. Concurrently, the objective function value of the problem (P1) has a lower bound, thereby ensuring the convergence of Algorithm 3.

IV. Numerical Results

In this section, we provide numerical results and simulations to rigorously evaluate the efficacy of the proposed AO-based algorithm. The positions of the HAP, the RIS 1, and RIS 2 are $(0,0)$, $(5,1)$, and $(15,1)$, respectively, while ZEDs are independently and uniformly distributed in a circular area centered at $(20,0)$ with radius 1 m. Unless otherwise stated, we deploy RIS 1 and RIS 2 near the HAP and the ZEDs, respectively. The large-scale path loss is modeled as $-30 - 10\alpha\log_{10}(d)$ dB, where α is the path loss exponent and d is the link distance. Specifically, α is set to 2.2 for the ZEDs cluster/HAP to nearby RIS link due to the short distance, and 3 for other longer-distance links, and the Rician factor is uniformly set to 3 dB. Table II presents the other system parameters unless otherwise specified. We illustrate the energy consumption performance through a comparative analysis of the proposed scheme (marked with "Proposed") and two benchmarks. For fair comparison, the total elements of RIS are 2 N. Our aim is to fully demonstrate the significant performance advantages of the proposed algorithm in the context of double zeRIS-assisted WP-MEC, thus we plot the following:

- Single RIS near HAP: a single RIS with random reflection coefficients, and RIS is located at $(5,1)$ [47].
- Random RIS reflection coefficients: Deploy two RISs with random reflection coefficients.
- Distributed two zeRISs: a scenario where two zeRISs are deployed without considering cascaded links.
- Proposed with $\mu = 5$ μW: the proposed cascaded system with $\mu = 5$ μW.
- Proposed: the proposed cascaded system with $\mu = 1$ μW.

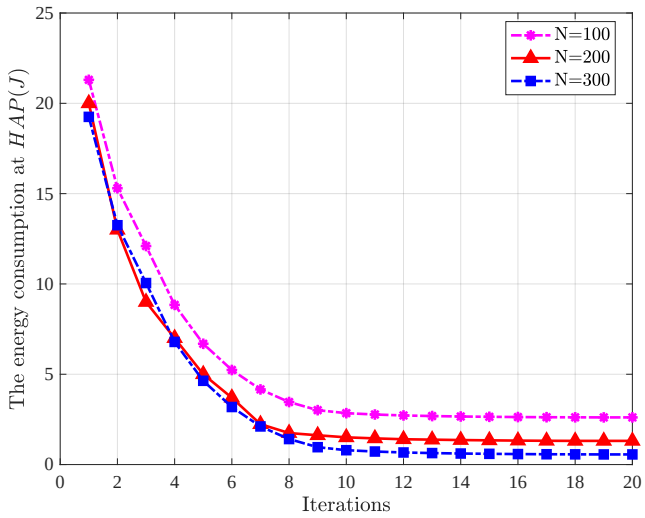

Fig. 3: Analysis of convergence in the proposed beamforming design algorithm

Fig. 3 shows the convergence performance of the proposed algorithm in a zeRIS-assisted WP-MEC system. The data presented in Fig. 3 depicts the decrease in HAP transmission energy with increasing iterations under different RIS reflection elements. We observe the proposed algorithm's rapid and stable convergence trend. This fact validates the algorithmic design's efficacy in zeRIS-assisted WP-MEC systems.

Fig.4 shows the total energy consumption versus the number of HAP antennas M, indicating that HAP transmission energy decreases as the number of antennas increases across different benchmarks. This trend is attributed to the increased spatial diversity gain associated with HAPs equipped with more antennas, thereby reducing the need for transmission energy.

This article has been accepted for publication in a future issue of this journal, but has not been fully edited. Content may change prior to final publication.
Citation information: DOI: 10.1109/TWC.2025.3581097, IEEE Transactions on Wireless Communications

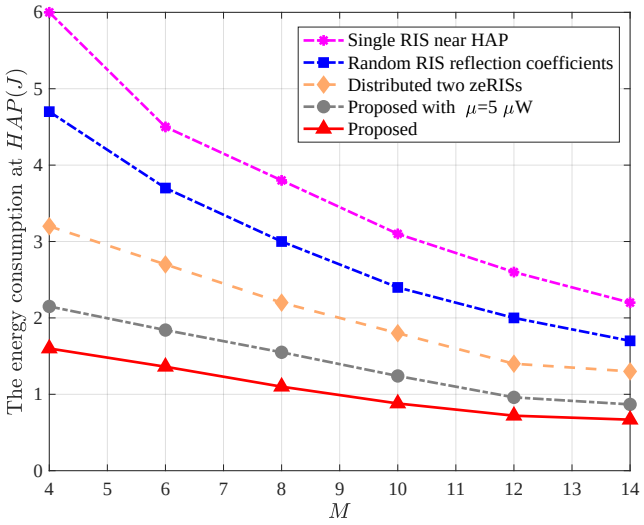

Fig. 4: The HAP energy consumption versus relative to M.

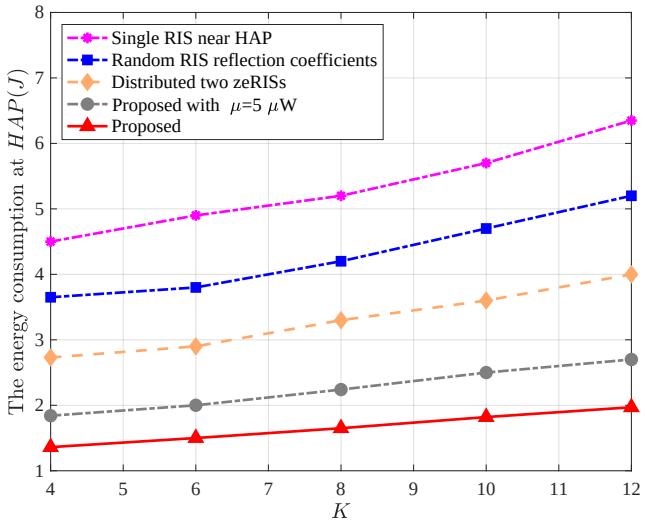

Fig. 6: The HAP energy consumption versus K.

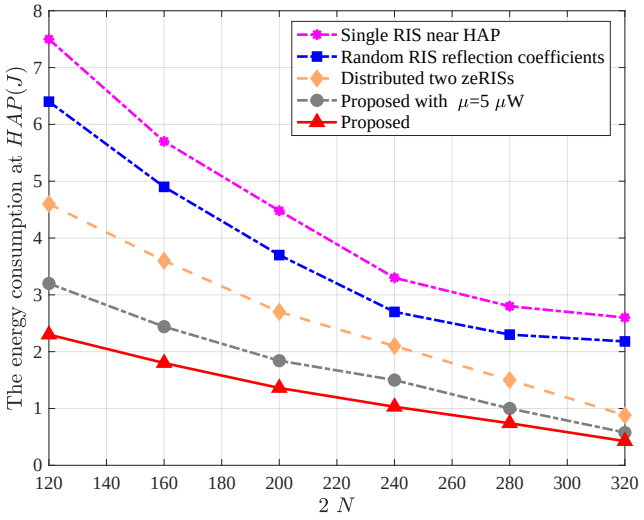

Fig. 5: The HAP energy consumption versus 2 N.

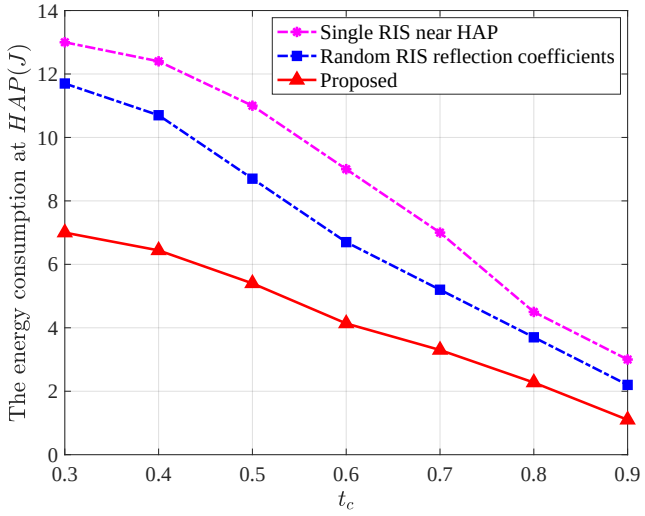

Fig. 7: The HAP energy consumption versus t_c.

Moreover, by comparing with the "Distributed two zeRISs" benchmark, it can be seen that the cascaded links between two zeRISs can further reduce the AP transmit power. Notably, when compared to systems with the same number of antennas, our algorithm outperforms other benchmarks, demonstrating the effectiveness of the zeRIS-assisted WP-MEC system and emphasizing the importance of strategic optimization in such systems.

Fig. 5 shows the energy consumption of the HAP decreases as the number of RIS elements N increases. Moreover, the performance of the proposed system under varying values of μ is also better than different benchmarks. Significantly, compared to single RIS-assisted WP-MEC, two-RIS-assisted WP-MEC requires fewer components to achieve the same target received power. This finding shows that the addition of RIS can help the WP-MEC system reduce energy consumption.

Fig. 6 shows the energy consumption of HAP versus the number of ZEDs for the comparison between the double- and single-RIS assisted WP-MEC systems. It can be observed from this figure that as the number of ZEDs within the HAP coverage area increases, the required transmission energy also rises. This is due to the HAP supplying more energy to meet the growing energy harvesting demands and computing workloads of additional ZEDs. Notably, for the same number of ZEDs, the proposed algorithm consistently outperforms the two benchmarks. Despite the rise in energy consumption attributed to the growing number of ZEDs, we observed that the "Proposed" solution showed the slowest energy consumption growth trend. This finding highlights the potential of zeRISs to balance energy efficiency and communication performance.

From the results obtained in Fig. 7, we can see that as the period t_c is extended, the overall energy consumption of the system is significantly reduced. This is because as t_c increases, $T - t_c$ decreases accordingly, allowing the HAP to meet the ZEDs' energy demands for task offloading in a shorter time. Thus, as t_c grows, the overall energy consumption of the system can be further reduced. While selecting a larger t_c appears advantageous, it may also result in a substantial

This article has been accepted for publication in a future issue of this journal, but has not been fully edited. Content may change prior to final publication.
Citation information: DOI: 10.1109/TWC.2025.3581097, IEEE Transactions on Wireless Communications

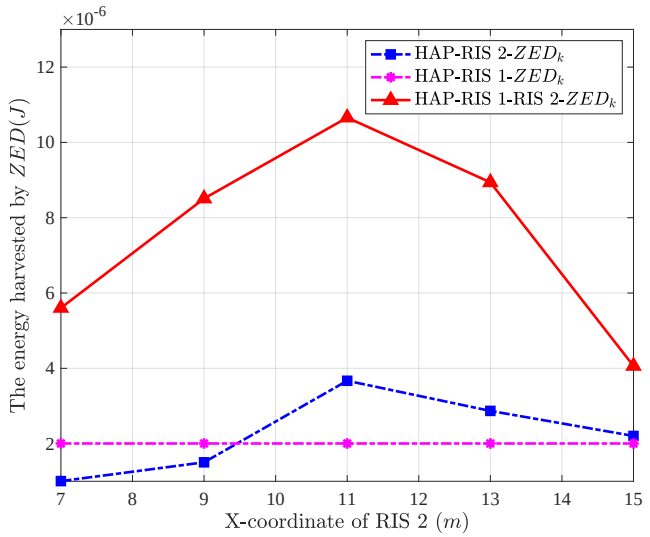

Fig. 8: The energy harvested by the ZEDs versus the position of RIS 2.

increase in UL power consumption. Therefore, as a trade-off, we recommend a maximum value of t_c of 0.9 for applications specific to the default settings [33].

Fig. 8 shows that the impact of RIS 2's location on the energy harvested by the ZED. The position of RIS 2 changes from 7 m to 15 m with a step size of 2 m. It can be observed that the energy harvested via the link HAP→RIS 1→RIS 2→k-th ZED is significantly higher than other single reflection links due to the passive beamforming gains between the two zeRISs. Moreover, the energy harvested by ZED initially increases and then decreases as RIS 2 moves away from the HAP, following the links HAP→RIS 1→RIS 2→k-th ZED and HAP→RIS 2→k-th ZED. This is because when RIS 2 is closer to both the HAP and RIS 1, the path loss of the signal before reaching RIS 2 is reduced, leading to lower energy consumption by the HAP. As the distance between RIS 2 and the HAP increases, the path loss for both $\mathbf{H}_2$ and $\mathbf{H}_{1,2}$ rises, requiring the HAP to increase its energy output to maintain sufficient signal strength at the ZEDs. Conversely, as RIS 2 moves closer to the ZEDs, it can more efficiently reflect the HAP signal towards the ZEDs, improving signal coverage and further reducing the HAP's energy consumption. These observations demonstrate the advantage of the proposed WP-MEC framework supported by two zeRISs, for zero-energy MEC networks.

V. Conclusion

This paper presented an energy minimization framework for WP-MEC networks supported by two zeRISs to enhance coverage, energy harvesting, and task offloading. During the energy harvesting period, ZEDs and two zeRISs harvested energy by using a nonlinear energy harvesting model to maintain self-sustainability. Then, an energy minimization algorithm was designed to optimize the key system parameters, including time allocation, HAP energy beamforming, and reflection coefficients for zeRISs, through mathematical solutions. The numerical results showed that the proposed algorithm significantly outperforms existing benchmarks. The use of two RISs saves at least 69% of the energy consumption compared to a single RIS. Future work will focus on adapting the algorithms to practical RIS hardware constraints, such as discrete phase shifts.

References

[1] S. Dang, O. Amin, B. Shihada, and M.-S. Alouini, "What should 6g be?" *Nature Electronics*, vol. 3, no. 1, pp. 20–29, 2020.
[2] N. A. Mitsiou, V. K. Papanikolaou, P. D. Diamantoulakis, and G. K. Karagiannidis, "Energy-aware optimization of zero-energy device networks," *IEEE Commun. Lett.*, vol. 26, no. 4, pp. 858–862, 2022.
[3] B. Clerckx, K. Huang, L. R. Varshney, S. Ulukus, and M.-S. Alouini, "Wireless power transfer for future networks: Signal processing, machine learning, computing, and sensing," *IEEE J. Sel. Areas Commun.*, vol. 15, no. 5, pp. 1060–1094, 2021.
[4] S. A. Tegos, G. K. Karagiannidis, P. D. Diamantoulakis, and N. D. Chatzidiamantis, "New results for pearson type III family of distributions and application in wireless power transfer," *IEEE Internet Things J.*, vol. 9, no. 23, pp. 24 038–24 050, Dec. 2022.
[5] J. Huang, Y. Zhou, Z. Ning, and H. Gharavi, "Wireless power transfer and energy harvesting: Current status and future prospects," *IEEE Wireless Commun.*, vol. 26, no. 4, pp. 163–169, 2019.
[6] Y. Huang and B. Clerckx, "Large-scale multiantenna multisine wireless power transfer," *IEEE Trans. Signal Process.*, vol. 65, no. 21, pp. 5812–5827, 2017.
[7] M. Hua, Q. Wu, W. Chen, O. A. Dobre, and A. L. Swindlehurst, "Secure intelligent reflecting surface-aided integrated sensing and communication," *IEEE Trans. Wirel. Commun.*, vol. 23, no. 1, pp. 575–591, 2024.
[8] C. Pan, G. Zhou, K. Zhi, S. Hong, T. Wu, Y. Pan, H. Ren, M. D. Renzo, A. Lee Swindlehurst, R. Zhang, and A. Y. Zhang, "An overview of signal processing techniques for RIS/IRS-aided wireless systems," *IEEE J. Sel. Top. Signal Process.*, vol. 16, no. 5, pp. 883–917, 2022.
[9] Q. Wu, B. Zheng, C. You, L. Zhu, K. Shen, X. Shao, W. Mei, B. Di, H. Zhang, E. Basar, L. Song, M. Di Renzo, Z.-Q. Luo, and R. Zhang, "Intelligent surfaces empowered wireless network: Recent advances and the road to 6G," *Proc. IEEE*, vol. 112, no. 7, pp. 724–763, 2024.
[10] Q. Wu and R. Zhang, "Intelligent reflecting surface enhanced wireless network via joint active and passive beamforming," *IEEE Trans. Wireless Commun.*, vol. 18, no. 11, pp. 5394–5409, 2019.
[11] C. Huang, R. Mo, and C. Yuen, "Reconfigurable intelligent surface assisted multiuser MISO systems exploiting deep reinforcement learning," *IEEE J. Sel. Areas Commun.*, vol. 38, no. 8, pp. 1839–1850, 2020.
[12] B. Zheng, C. You, and R. Zhang, "Double-IRS assisted multi-user MIMO: Cooperative passive beamforming design," *IEEE Trans. Commun.*, vol. 20, no. 7, pp. 4513–4526, 2021.
[13] Z. Chu, J. Zhong, P. Xiao, D. Mi, W. Hao, R. Tafazolli, and A. P. Feresidis, "RIS assisted wireless powered IoT networks with phase shift error and transceiver hardware impairment," *IEEE Trans. Commun.*, vol. 70, no. 7, pp. 4910–4924, 2022.
[14] Q. Wu, X. Guan, and R. Zhang, "Intelligent reflecting surface-aided wireless energy and information transmission: An overview," *Proc. IEEE*, vol. 110, no. 1, pp. 150–170, 2022.
[15] D. Tyrovolas, S. A. Tegos, V. K. Papanikolaou, Y. Xiao, P.-V. Mekikis, P. D. Diamantoulakis, S. Ioannidis, C. K. Liaskos, and G. K. Karagiannidis, "Zero-energy reconfigurable intelligent surfaces (zeRIS)," *IEEE Trans. Wireless Commun.*, pp. 1–1, 2023.
[16] Y. Pan, K. Wang, C. Pan, H. Zhu, and J. Wang, "Self-sustainable reconfigurable intelligent surface aided simultaneous terahertz information and power transfer (STIPT)," *IEEE Trans. Wireless Commun.*, vol. 21, no. 7, pp. 5420–5434, 2022.
[17] Z. Chu, P. Xiao, D. Mi, W. Hao, Y. Xiao, and L.-L. Yang, "Multi-IRS assisted multi-cluster wireless powered IoT networks," *IEEE Trans. Wireless Commun.*, 2022.
[18] C. Kumar and S. Kashyap, "On the power transfer efficiency and feasibility of wireless energy transfer using Double IRS," *IEEE Trans. Veh. Technol.*, vol. 72, no. 5, pp. 6165–6180, 2023.
[19] D. Tyrovolas, S. A. Tegos, E. C. Dimitriadou-Panidou, P. D. Diamantoulakis, C. K. Liaskos, and G. K. Karagiannidis, "Performance analysis of cascaded reconfigurable intelligent surface networks," *IEEE Wireless Commun. Lett.*, vol. 11, no. 9, pp. 1855–1859, 2022.

This article has been accepted for publication in a future issue of this journal, but has not been fully edited. Content may change prior to final publication.
Citation information: DOI: 10.1109/TWC.2025.3581097, IEEE Transactions on Wireless Communications

[20] N. G. Evgenidis, N. A. Mitsiou, V. I. Koutsioumpa, S. A. Tegos, P. D. Diamantoulakis, and G. K. Karagiannidis, "Multiple access in the era of distributed computing and edge intelligence," *Proc. IEEE*, pp. 1–30, 2024.

[21] T. Bai, C. Pan, C. Han, and L. Hanzo, "Reconfigurable intelligent surface aided mobile edge computing," *IEEE Wireless Commun.*, vol. 28, no. 6, pp. 80–86, 2021.

[22] T. Bai, C. Pan, Y. Deng, M. Elkashlan, A. Nallanathan, and L. Hanzo, "Latency minimization for intelligent reflecting surface aided mobile edge computing," *IEEE J. Sel. Areas Commun.*, vol. 38, no. 11, pp. 2666–2682, 2020.

[23] P. D. Diamantoulakis, P. S. Bouzinis, P. G. Sarigannidis, Z. Ding, and G. K. Karagiannidis, "Optimal design and orchestration of mobile edge computing with energy awareness," *IEEE Trans. Sustain. Comput.*, vol. 7, no. 2, pp. 456–470, 2022.

[24] F. Jiang, Y. Peng, K. Wang, L. Dong, and K. Yang, "MARS: A DRL-based multi-task resource scheduling framework for UAV with IRS-assisted mobile edge computing system," *IEEE Trans. Cloud Comput.*, vol. 11, no. 4, pp. 3700–3712, 2023.

[25] B. Li, W. Wu, Y. Li, and W. Zhao, "Intelligent reflecting surface and artificial-noise-assisted secure transmission of MEC system," *IEEE Internet Things J.*, vol. 9, no. 13, pp. 11 477–11 488, 2022.

[26] W. He, D. He, X. Ma, X. Chen, Y. Fang, and W. Zhang, "Joint user association, resource allocation, and beamforming in RIS-assisted multi-server MEC systems," *IEEE Trans. Wireless Commun.*, pp. 1–1, 2023.

[27] Z. Chen, J. Tang, M. Wen, Z. Li, J. Yang, X. Y. Zhang, and K.-K. Wong, "Reconfigurable intelligent surface assisted MEC offloading in NOMA-enabled iot networks," *IEEE Trans. Commun.*, vol. 71, no. 8, pp. 4896–4908, 2023.

[28] X. Hu, C. Masouros, and K.-K. Wong, "Reconfigurable intelligent surface aided mobile edge computing: From optimization-based to location-only learning-based solutions," *IEEE Trans. Commun.*, vol. 69, no. 6, pp. 3709–3725, 2021.

[29] Y. Zhou, C. Pan, P. L. Yeoh, K. Wang, Z. Ma, B. Vucetic, and Y. Li, "Joint optimization for cooperative computing framework in Double-IRS-aided MEC systems," *IEEE Wireless Commun. Lett.*, vol. 12, no. 5, pp. 779–783, 2023.

[30] F. Wang, J. Xu, X. Wang, and S. Cui, "Joint offloading and computing optimization in wireless powered mobile-edge computing systems," *IEEE Trans. Wireless Commun.*, vol. 17, no. 3, pp. 1784–1797, 2018.

[31] C. You, K. Huang, and H. Chae, "Energy efficient mobile cloud computing powered by wireless energy transfer," *IEEE J. Sel. Areas Commun.*, vol. 34, no. 5, pp. 1757–1771, 2016.

[32] X. Qin, Z. Song, T. Hou, W. Yu, J. Wang, and X. Sun, "Joint resource allocation and configuration design for STAR-RIS-enhanced wireless-powered MEC," *IEEE Trans. Commun.*, vol. 71, no. 4, pp. 2381–2395, 2023.

[33] T. Bai, C. Pan, H. Ren, Y. Deng, M. Elkashlan, and A. Nallanathan, "Resource allocation for intelligent reflecting surface aided wireless powered mobile edge computing in OFDM systems," *IEEE Trans. Wireless Commun.*, vol. 20, no. 8, pp. 5389–5407, 2021.

[34] S. Zargari, C. Tellambura, and S. Herath, "Energy-efficient hybrid offloading for backscatter-assisted wirelessly powered MEC with reconfigurable intelligent surfaces," *IEEE Trans. Mobile Comput.*, vol. 22, no. 9, pp. 5262–5279, 2023.

[35] H. Li, K. Xiong, R. Dong, P. Fan, and K. Ben Letaief, "Joint active and passive beamforming in IRS-enhanced wireless powered MEC networks," *IEEE Wireless Commun. Lett.*, vol. 11, no. 11, pp. 2285–2289, 2022.

[36] S. Mao, N. Zhang, L. Liu, J. Wu, M. Dong, K. Ota, T. Liu, and D. Wu, "Computation rate maximization for intelligent reflecting surface enhanced wireless powered mobile edge computing networks," *IEEE Trans. Veh. Technol.*, vol. 70, no. 10, pp. 10 820–10 831, 2021.

[37] Q. Wu and R. Zhang, "Joint active and passive beamforming optimization for intelligent reflecting surface assisted SWIPT under qos constraints," *IEEE J. Sel. Areas Commun.*, vol. 38, no. 8, pp. 1735–1748, 2020.

[38] Z. Chu, P. Xiao, M. Shojafar, D. Mi, W. Hao, J. Shi, and F. Zhou, "Utility maximization for IRS assisted wireless powered mobile edge computing and caching (WP-MECC) networks," *IEEE Trans. Commun.*, vol. 71, no. 1, pp. 457–472, 2022.

[39] G. Chen, Q. Wu, W. Chen, D. W. K. Ng, and L. Hanzo, "IRS-aided wireless powered MEC systems: TDMA or NOMA for computation offloading?" *IEEE Trans. Wireless Commun.*, vol. 22, no. 2, pp. 1201–1218, 2022.

[40] P. Chen, B. Lyu, Y. Liu, H. Guo, and Z. Yang, "Multi-IRS assisted wireless-powered mobile edge computing for internet of things," *IEEE Trans. Green Commun. Netw.*, vol. 7, no. 1, pp. 130–144, 2023.

[41] N. Li, W. Hao, F. Zhou, Z. Chu, S. Yang, and P. Xiao, "Resource management for IRS-assisted WP-MEC networks with practical phase shift model," *IEEE Internet Things J.*, 2023.

[42] G. Li, M. Zeng, D. Mishra, L. Hao, Z. Ma, and O. A. Dobre, "Latency minimization for IRS-aided NOMA MEC systems with WPT-enabled iot devices," *IEEE Internet Things J*, 2023.

[43] H. An Le, T. Van Chien, V. D. Nguyen, and W. Choi, "Double RIS-assisted MIMO systems over spatially correlated rician fading channels and finite scatterers," *IEEE Trans. Commun.*, vol. 71, no. 8, pp. 4941–4956, Aug. 2023.

[44] G. Zhou, C. Pan, H. Ren, P. Popovski, and A. L. Swindlehurst, "Channel estimation for RIS-aided multiuser millimeter-wave systems," *IEEE Trans. Signal Process.*, vol. 70, pp. 1478–1492, 2022.

[45] G. Zhou, C. Pan, H. Ren, K. Wang, and A. Nallanathan, "A framework of robust transmission design for IRS-aided MISO communications with imperfect cascaded channels," *IEEE Trans. Signal Process.*, vol. 68, pp. 5092–5106, 2020.

[46] C. You, B. Zheng, and R. Zhang, "Wireless communication via double IRS: Channel estimation and passive beamforming designs," *IEEE Wireless Commun. Lett.*, vol. 10, no. 2, pp. 431–435, 2020.

[47] Y. Zheng, S. A. Tegos, Y. Xiao, P. D. Diamantoulakis, Z. Ma, and G. K. Karagiannidis, "Zero-energy device networks with wireless-powered RISs," *IEEE Trans. Veh. Technol.*, pp. 1–5, 2023.

[48] Z. Li, W. Chen, Q. Wu, H. Cao, K. Wang, and J. Li, "Robust beamforming design and time allocation for IRS-assisted wireless powered communication networks," *IEEE Trans. Commun.*, vol. 70, no. 4, pp. 2838–2852, 2022.

[49] Y. Zou, Y. Long, S. Gong, D. T. Hoang, W. Liu, W. Cheng, and D. Niyato, "Robust beamforming optimization for self-sustainable intelligent reflecting surface assisted wireless networks," *IEEE Trans. Cogn. Commun. Netw.*, vol. 8, no. 2, pp. 856–870, 2021.

[50] S. Zargari, A. Hakimi, C. Tellambura, and S. Herath, "Multiuser MISO PS-SWIPT systems: Active or passive RISs?" *IEEE Wireless Commun. Lett.*, vol. 11, no. 9, pp. 1920–1924, 2022.

[51] K. Zheng, G. Jiang, X. Liu, K. Chi, X. Yao, and J. Liu, "DRL-based offloading for computation delay minimization in wireless-powered multi-access edge computing," *IEEE Trans. Commun.*, vol. 71, no. 3, pp. 1755–1770, 2023.

[52] M. Wu, Q. Song, L. Guo, and I. Lee, "Energy-efficient secure computation offloading in wireless powered mobile edge computing systems," *IEEE Trans. Veh. Technol.*, vol. 72, no. 5, pp. 6907–6912, 2023.

[53] M. Grant and S. Boyd, "CVX: Matlab software for disciplined convex programming, version 2.1," Mar. 2014, [Online].

Luyao Zhang received the master's degree in Operations Research and Cybernetics from Southwest University. She is currently pursuing the Ph.D. degree in information and communication engineering with Southwest Jiaotong University. She was a Visiting Ph.D. Student with the Aristotle University of Thessaloniki, Greece, from 2024 to 2025. Her research interests include wireless power transfer and wireless communication networks.

Yi Zhou (Member, IEEE) received her Ph.D. degree from University of Sydney, Australia, in 2020. Since 2021, she has been with School of Information Science and Technology, Southwest Jiaotong University, China. Her research interests include physical layer security, UAV communications, and 5G related communications. She was a recipient of the Postgraduate Scholarship and the Norman I. Price Scholarship from the Center of Excellence in Telecommunications, School of Electrical and Information Engineering, University of Sydney. She was a recipient of Marie Skłodowska Curie Postdoctoral Fellowship.

This article has been accepted for publication in a future issue of this journal, but has not been fully edited. Content may change prior to final publication.
Citation information: DOI: 10.1109/TWC.2025.3581097, IEEE Transactions on Wireless Communications

Sotiris A. Tegos (Senior Member, IEEE) received the Diploma (5 years) and the Ph.D. degree from the Department of Electrical and Computer Engineering, Aristotle University of Thessaloniki, Thessaloniki, Greece, in 2017 and 2022, respectively. Since 2022, he is a Postdoctoral Fellow with the Wireless Communications and Information Processing (WCIP) Group, Aristotle University of Thessaloniki. In 2018, he was a visitor researcher at the Department of Electrical and Computer Engineering at Khalifa University, Abu Dhabi, UAE. His current research interests include multiple access in wireless communications, wireless power transfer, and optical wireless communications. He serves as an Editor for IEEE Transactions on Communications and IEEE Communications Letters. He received the Best Paper Award in 2023 Photonics Global Conference (PGC) and in 2025 IEEE Wireless Communications and Networking Conference (WCNC). He was an exemplary reviewer in IEEE Wireless Communications Letters in 2019, 2022 and 2023 (top 3% of reviewers) and an exemplary Editor in IEEE Communications Letters in 2024.

Yu Zheng received the B.Sc. and Ph.D. degrees in communication engineering from Southwest Jiaotong University, Chengdu, China, in 2015 and 2024, respectively. He is currently a postdoctoral in the Department of Automation, Tsinghua University. His research interests include DOA estimation, antenna design, vital signs monitoring, mmwave radar signal processing, and wireless communications.

Panagiotis D. Diamantoulakis (Senior Member, IEEE) received the Diploma (5 years) and the Ph.D. degree from the Department of Electrical and Computer Engineering, Aristotle University of Thessaloniki, Thessaloniki, Greece, in 2012 and 2017, respectively. From 2017 to 2024, he was a Postdoctoral Fellow with Wireless Communications and Information Processing (WCIP) Group, AUTH and since 2021, he has been a Visiting Assistant Professor with the Key Lab of Information Coding and Transmission, Southwest Jiaotong University, Chengdu, China. In May 2024, he joined the faculty of the Aristotle University of Thessaloniki, Greece, where he is currently Assistant Professor at the Department of Electrical and Computer Engineering. His research interests include optimization theory and applications in wireless networks, optical wireless communications, and goal-oriented communications. He serves as an Editor of IEEE Open Journal of the Communications Society, while during 2018-2023 he has been an Editor of IEEE Wireless Communications Letters, in which he was an Exemplary Editor of the IEEE Wireless Communications Letters in 2020. Also, he was an Exemplary Reviewer of the IEEE Communications Letters in 2014 and the IEEE Transactions on Communications in 2017 and 2019 (top 3% of reviewers).

Li Hao (Member, IEEE) received the Ph.D. degree in transportation information engineering and controlling from Southwest Jiaotong University, Chengdu, China, in 2003. She is currently a Professor with the School of Information Science and Technology, Southwest Jiaotong University. Her research interests include information theory & coding, 5G/B5G communications, cooperative communications, and low-power IoT communications. She is currently the Deputy Director of communication and signaling branch of China Railway Society.

George K. Karagiannidis (Fellow, IEEE) received the Ph.D. degree in Telecommunications Engineering from Electrical Engineering Department, University of Patras, Greece, in 1998. He is currently a Professor with the Electrical and Computer Engineering Department, Aristotle University of Thessaloniki, Thessaloniki, Greece, and the Head of Wireless Communications and Information Processing (WCIP) Group. His research interests are in the areas of wireless communications systems and networks, signal processing, optical wireless communications, wireless power transfer, and signal processing for biomedical engineering. Dr. Karagiannidis recently received three prestigious awards: The 2021 IEEE ComSoc RCC Technical Recognition Award, the 2018 IEEE ComSoc SPCE Technical Recognition Award, and the 2022 Humboldt Research Award from Alexander von Humboldt Foundation. He is one of the Highly Cited Authors across all areas of Electrical Engineering, recognized from Clarivate Analytics as the Web-of-Science Highly-Cited Researcher in the ten consecutive years 2015–2024. Currently, he is the Editor-in Chief of IEEE Transactions on Communications and in the past was the Editor-in Chief of IEEE Communications Letters.